Deltares

Enabling Delta Life

Hydrodynamic validation of Delft3D using data from the SandyDuck97 experiments

Hydrodynamic validation of Delft3D using data from the SandyDuck97 experiments

Jebbe van der Werf

Prepared for:

Rijkswaterstaat Waterdienst

Hydrodynamic validation of Delft3D using data from the SandyDuck97 measurements

Jebbe van der Werf

Report Z4582.17

February 2009

Client	Rijkswaterstaat Waterdienst
Title	Hydrodynamic validation of Delft3D using data from the SandyDuck97 measurements

Abstract

This report describes a hydrodynamic validation of Delft3D using data from the SandyDuck97 field measurements. 46 different cases are modelled with Delft3D; both in two-dimensional horizontal (2DH) and in three-dimensional (3D) mode. Measured and computed wave heights and current velocities are compared along a cross-shore transect across the surf zone. The sensitivity of the 2DH runs to the Chézy roughness coefficient, horizontal background viscosity, breaker delay and wave breaker coefficient α has been investigated. Furthermore, the effect of the number and distribution of the vertical computational layers and the vertical turbulence model have been studied with the 3D model. Finally, the results from the 2DH and 3D model are intercompared.

Wave heights computed with the calibrated 2DH model agree reasonably well with the measured data. However, wave heights are systematically overpredicted, which could be related to the absence of wave dissipation due to bottom friction in the roller model. On average, the 2DH model does well in predicting current velocities, but it overpredicts in deep water and underpredicts in shallow water. Furthermore, it overpredicts the longshore current maxima and underpredicts the distance of these maxima to the shore. The longshore current predictions with the 3D model are very sensitive to the adopted turbulence model and the thickness of the lowest computational layer. The thinner this layer, the lower the longshore currents. This is related to the way the bed shear stress is calculated. Depth-averaged currents computed by the 3D model are systematically lower than those computed by the 2DH model. Therefore, a 3D model based on a 2DH model needs to be re-calibrated hydrodynamically. The re-calibrated 3D model performs worse than the 2DH model in predicting the longshore currents and the location of the longshore current maxima, but does better in predicting the magnitude of the longshore current maxima. Based on these findings, a number of model improvements and further model investigations are proposed.

References	

Ver	Author	Date	Remarks	Review	Approved by
1	Jebbe van der Werf	10 December 2008		Maarten van Ormondt	
2	Jebbe van der Werf	18 February 2009		Maarten van Ormondt	Tom Schilperoort

Project number	Z4582.17
Keywords	
Number of pages	44
Classification	None
Status	Final

Contents

Chapter 1 Introduction

1.1 Background

The question of sand transport and the resulting morphological evolution of the coastal zone is fundamental to all major coastal management, coastal defence and coastal environment policies. Delft3D, a coastal area modelling tool, is commonly used by coastal engineering practitioners to model coastal environments, e.g. to study the morphological behaviour of a shoreface nourishment (see e.g. Walstra et al, 2008).

Delft3D is continuously in development. In recent years, Delft3D has been updated such that it now includes the following modules:

1 depth-dependent expression for γ (ratio of maximum wave height and water depth) of Ruessink et al. (2003),

2 surface roller model (see Reniers et al., 2004),

3 the breaker delay concept of Roelvink et al. (1995),

4 surf beat model (see Reniers et al., 2004),

5 the TRANSPOR2004 sediment transport model of Van Rijn (2007a,b,c).

These modules have not yet been evaluated thoroughly using field data.

Walstra et al. (2008) applied the updated Delft3D (without surf beat) to study the morphodynamics of a shoreface nourishment at Egmond aan Zee, The Netherlands. Delft3D, in area mode, was unable to make predictions on longer time scales (years) due to the development of small-scale longshore undulations which after some time affected the entire surf zone domain. These instabilities along the shoreline are not realistic and appear to be due to, among other things, an underestimation of the wave-driven longshore current close to the shore. As the model was not compared with measurements of wave dynamics, hydrodynamics or sediment dynamics there is not certainty about what is causing these instabilities. This underlines the general need to thoroughly validate newly-implemented modules in Delft3D.

The Duck94 (Birkemeier and Thornton, 1994) and SandyDuck97 experiments are large field campaigns at the Field Research Facility (FRF) located in Duck, North Carolina, USA. Wave dynamics, hydrodynamics, sediment dynamics and morphodynamics were measured in detail in the nearshore zone during about one month. During the test period, the wave climate included calm and storm periods, and substantial bathymetry changes occurred. This makes these two field experiments very useful to assess Delft3D for the nearshore environment. Furthermore, these data sets have already been used in the past to evaluate the performance of Delft3D by Hsu et al. (2006, 2008) and others.

Hsu et al. (2006) investigated the effects of many parameters and options on the performance of Delft3D using Duck94 and NSTS Santa Barbara data. For the Duck94 cases they set up a two-dimensional horizontal (2DH) model. They concluded that (i) all

bottom friction formulations produced good longshore currents if proper friction coefficients are taken, (ii) the inclusion of roller improved the longshore current prediction, (iii) the Ruessink et al.'s (2003) γ-expression provided better results than the default fixed γ setting, (iv) including breaker delay improved longshore current prediction at Duck94, but worsened the longshore current prediction at Santa Barbara beach, (v) roller stress should be turned off at shallow depth (0.4 m) to avoid spuriously high currents.

As a follow up of this study, Hsu et al. (2008) extended the validation of Delft3D (in 2DH mode) with the SandyDuck97 data. They chose the model parameters on the basis of their earlier study, and compared in more detail measured and simulated wave heights and longshore currents. They recommended the following model set-up: (i) roller on, (ii) variable gamma, (iii) Chézy roughness with a value between 65 to 70 $m^{1/2}/s$ (iv) roller stress turned off at 0.4 m, and v) Neumann boundary conditions for flow side boundaries.

Furthermore, they showed that differences between with and without wave-current interactions for longshore currents and waves are not significant. It should be noted that rip current cases were excluded from the comparison. Hsu et al. (2006,2008) did not look into three-dimensional (3D) effects, which will be the focus of this study.

1.2 Objective

The overall objective of this study is to evaluate:

1 the capability of Delft3D to predict the nearshore wave and flow field,

2 the sensitivity of these predictions to different model options, and

3 the differences between the nearshore flow field predicted by Delft3D in fully 3D and 2DH mode

on the basis of data from the SandyDuck97 experiments.

1.3 Research methodology

First, we will set-up a 2DH model of the SandyDuck97 cases on the basis of the model created by Hsu et al. (2006, 2008). Then we will study the model sensitivity and optimize the model settings based on the measured wave heights and longshore current velocities. Next, we will set-up the 3D model, test the sensitivity of this model to the turbulence model and the number of vertical computational layers, and optimize longshore current predictions by varying the Chézy roughness coefficient. Finally, we will compare the 2DH and the 3D model results.

1.4 Outline of the report

This report is organized as follows. Chapter 2 gives a short description of the SandyDuck97 field campaign and the experimental conditions. The next chapter discusses how the SandyDuck97 cases are modelled with Delft3D. Computational results are compared with the measurements in Chapter 4. In the final chapter the conclusions are presented along with recommendations for further research.

Chapter 2 The SandyDuck97 experiments

2.1 Introduction

The SandyDuck97 experiments were conducted at the Field Research Facility (FRF) located in Duck, North Carolina, USA. Duck94 (August and October 1994) was designed as a pilot effort to test instruments and procedures required for the more comprehensive SandyDuck97 experiment (October 1997). Figure 2.1 shows the location of FRF.

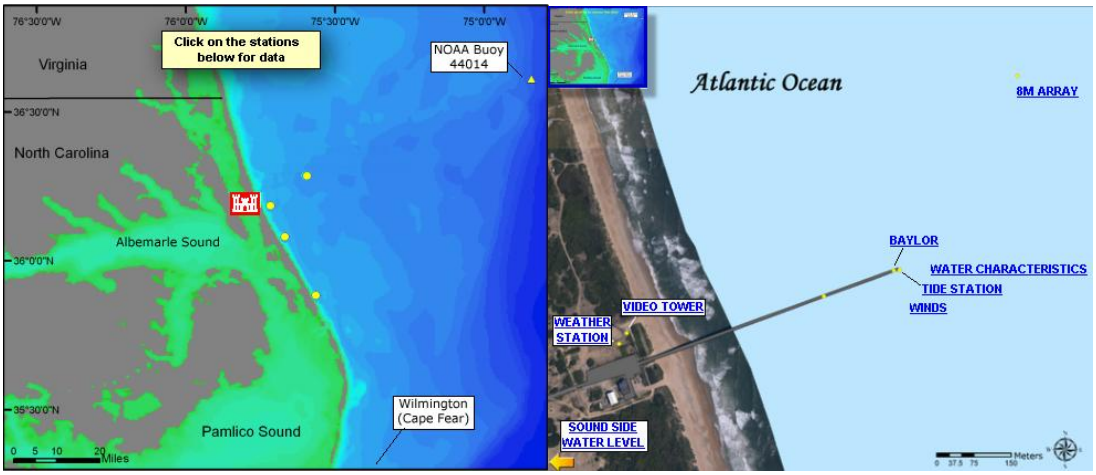

Figure 2.1 Location of the Field Research Facility (FRF) (denoted with a castle in the left panel) and the measuring pier. (taken from http://www.frf.usace.army.mil)

At the Duck site, waves are generally from the South in Augustus and variable in October with usually the largest waves from the North owing to Northeasters. The morphology tends to be three-dimensional with crescentic bars except during times of large waves when the inner bar is linear. Based on five years of statistics, the mean shorelines in August and October are located at 104±6 m and 110±8 m (in FRF coordinates, see Section 2.2) with the mean inner bar locations at 61±22 m and 82±26 m from the shoreline (Birkemeier and Thornton, 1994). The longshore influence of the FRF pier on the shoreline in the experimental area varies from year to year, but is greatest during August as a result of the consistently southerly approaching waves. The influence is much less during October following the corrective action of waves from the Northeast. The mean grain size during these months is a bimodal mixture of coarse and medium sand on the foreshore, fine in the surf zone (0.2 mm) and finer offshore (Birkemeier and Thornton, 1994).

2.2 Description of the data

Instruments are located by their latitude and longitude and by their position in the FRF coordinate System. The origin of this system is the intersection of a shore-parallel baseline with the southern boundary of the FRF property. Positive directions are toward the North (longshore) and offshore (cross-shore). The *z*-axis (vertical) is positive upwards and is relative to NGVD (National Geodetic Vertical Datum). This datum is 0.42 m above Mean Low Water (MLW).

During the SandyDuck field campaign extensive nearshore measurements were made of the bed elevation, bed forms, water surface elevation, water surface slope, flow

velocities, sediment concentrations and temperature at different horizontal and vertical positions using various instruments based on different measurement principles. Central to the surf zone array are SPUVT instrument frames each containing a sonar altimeter (S), pressure gage (P), bi-directional current meter (UV) and thermistor (T). These were deployed in multiple lines, and at varying spacing, in order to measure nearshore dynamics and bed level changes in both cross-shore and longshore directions. Figure 2.2 shows the locations of these frames (circles), as well as the location of other frames (triangles).

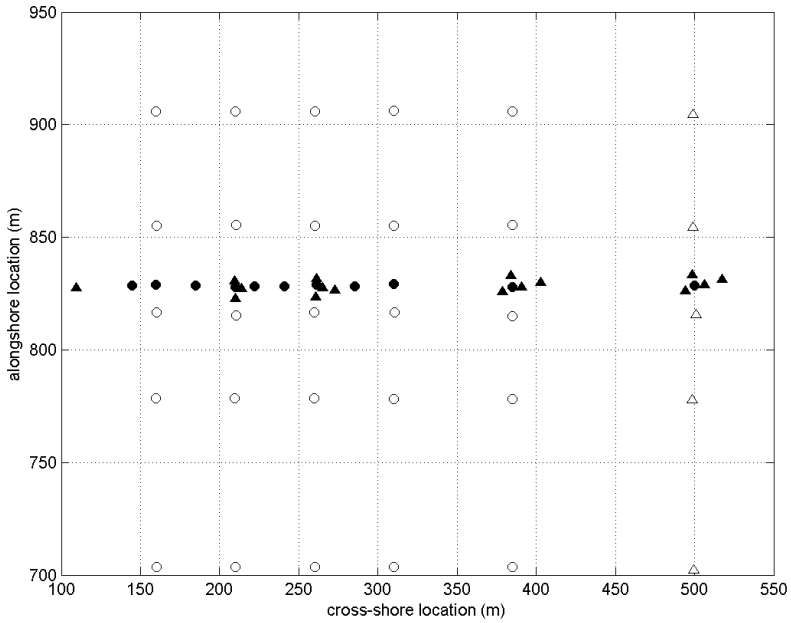

Figure 2.2 Locations of combined wave height and current measurements (circles) and only wave height measurements (triangles). Closed symbols indicate the locations of the measurements from which data are used in the present study.

The SPUVT data as well as the other data from measurements locations shown in Figure 2.2 were sampled at 2 Hz for 10784 s every 3 hours (10800 s). Collection times started at 0100 EST (Eastern Standard Time) and were repeated every 3 hours. Significant wave height data were computed from the sea-surface elevations in the frequency band 0.05 to 0.25 Hz based on record length of 1024 s. The same periods were used to compute the mean and the variance of the cross- and longshore currents. Sonar bottom positions are 3 hr averages of the 2 Hz data, and are relative to NGVD.

In our comparisons below we focus on the central transect, i.e. at $y \approx$ 830 m, along which 27 pressure sensors and 11 current meters were located. In the period on which we focus (09/27 – 10/20) the vertical positions of the current meters with respect to the vertical datum (NGVD) were constant. Due to morphological changes, the elevation of the current meters above the bed varied. Table 2.1 shows for each current meter the horizontal coordinates, the mean sensor elevation above the bed (absolute and relative to the water depth) and the standard deviation of the sensor elevation above the bed (absolute and relative to the water depth). The effect of the vertical tide on the water depth is not accounted for.

Table 2.1 Horizontal and vertical positions of the current meters used for model-data comparison.

Current meter	*X* (m)	*Y* (m)	mean(*z*) (m)	std(*z*) (m)	mean (*z*/*h*)	std(*z*/*h*)
1	144.8	828.4	0.39	0.15	0.34	0.10
2	159.8	828.8	0.64	0.20	0.57	0.08
3	184.8	828.7	0.35	0.18	0.20	0.09
4	209.9	827.9	0.96	0.08	0.32	0.02
5	222.0	828.4	0.90	0.02	0.27	0.01
6	240.7	828.4	0.74	0.03	0.20	0.01
7	261.2	828.8	0.68	0.04	0.19	0.01
8	285.6	828.7	0.65	0.06	0.18	0.01
9	310.1	829.4	0.70	0.04	0.20	0.01
10	384.8	827.9	1.05	0.03	0.26	0.01
11	500.2	828.6	0.93	0.04	0.17	0.01

This table shows that the variance in sensor position relative to the bed is larger for the more shoreward located sensors, as a result of larger morphological changes. On average the sensors are located between 0.2 and 0.6 times the water depth above the bed. For a logarithmic current profile, which is a reasonable assumption for the longshore current, the current at $z = h/e \approx 0.4h$ equals the depth-averaged value. Therefore, as a first step, it seems justified to compare computed depth-averaged velocities with velocities measured at a certain elevation above the bed, as we will do below for the 2DH model.

To model the SandyDuck cases we further use the following data.

- Directional wave data from a nine element linear array of bottom mounted pressure gages located on the 8 m contour about 900 m offshore of FRF. The data were collected at 2 Hz; statistics are computed from 8192 s intervals.

- Tidal data from the National Oceanic and Atmospheric Administration (NOAA) primary tide station located at the seaward end of the FRF pier (vertical tide every 6 minutes).

- Meteorological data collected relatively close to the experimental area; 34-minute statistics of wind speed and wind direction.

- The Coastal Research Amphibious Buggy (CRAB) was used to collect daily maps of the bathymetry surrounding the instruments in an area known as the minigrid. If the conditions allowed, a series of 18 profile lines were surveyed regularly throughout the experiment. The lines were spaced approximately 25 m apart near the instruments and 50 m apart elsewhere. All lines extended from the base of the dune to approximately 400 m offshore. The dune section of each profile line was only surveyed at the beginning of the experiment. To provide continuity between surveys, the dune data points were automatically added to each survey.

- A bathymetric survey for a much larger area at a coarser spacing was conducted every other month.

2.3 Conditions

The figures below show the water level, wind speed, wind direction, significant wave height, spectral peak period and peak wave direction from 27th September to 21st October 1997. The wind direction is defined nautically; 0° denotes wind coming from the North and positive in clockwise direction. The wave direction represents the angle in degrees counter-clockwise from normal to the array, or approximately shore normal to the *x*-axis; i.e. +90° means waves coming from the North.

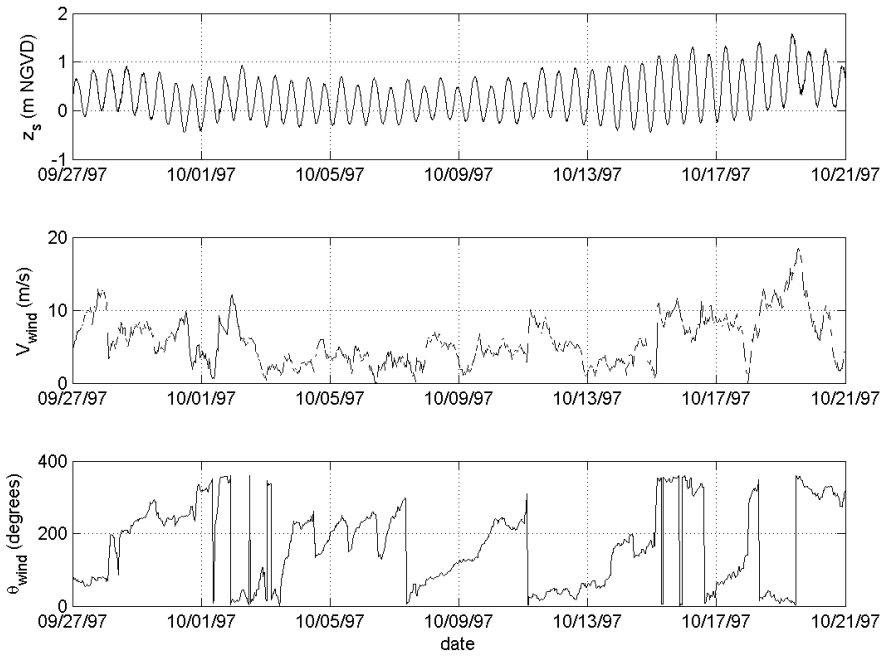

Figure 2.3 Water elevation, wind speed and wind direction during SandyDuck97 field campaign. The wind direction is defined nautically and positive in clockwise direction.

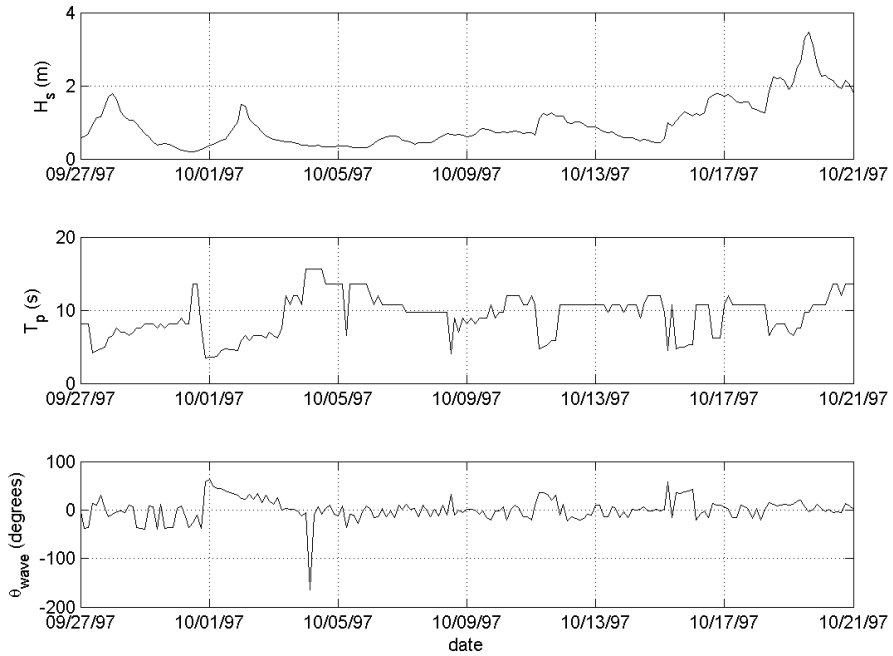

Figure 2.4 Significant wave height, spectral peak period and wave direction during SandyDuck97 field campaign. The wave direction represents the angle in degrees counter-clockwise from shore normal.

The water elevation shows the dominance of a M2 tide with an amplitude of about 0.5 m. Incident wave height varied from calm (< 0.5 m) to a short-lived peak of just over 3.5 m during the "SandyDuck storm" occurring between 18 and 21 October.

2.4 Selected SandyDuck cases

We focus on the same 46 cases as Hsu et al. (2008) did. Cases with low waves (less than 0.6 m) or rip currents were not included. These cases are listed below with for each case the vertical tidal level, the magnitude of the wind velocity, the significant wave height, the spectral peak period and the direction of the spectral wave peak.

Table 2.2 The vertical water level, wind and wave conditions of the 46 selected SandyDuck cases.

Date and time	Z_{tide} (m NGVP)	V_{wind} (m/s)	θ_{wind} (^{o})	H_s (m)	T_p (s)	θ_{Tp} (^{o})
09/27 19:00:00	0.64	10.7	70.6	1.43	5.0	4.0
09/27 22:00:00	0.06	11.8	78.6	1.69	6.2	-14.0
09/28 01:00:00	0.24	12.5	77.0	1.79	6.6	-8.0
09/28 04:00:00	0.81	3.4	101.5	1.63	7.6	-4.0
09/28 07:00:00	0.64	5.8	194.7	1.28	7.0	-2.0
09/28 10:00:00	0.08	5.9	147.0	1.14	7.0	-6.0
09/28 13:00:00	0.23	8.3	202.1	1.06	6.6	10.0
09/28 16:00:00	0.78	7.6	209.2	1.07	7.0	6.0
09/28 19:00:00	0.79	5.3	203.7	0.96	7.6	-36.0
10/02 01:00:00	-0.20	11.1	16.8	1.49	5.8	24.0
10/02 04:00:00	0.28	8.7	17.1	1.43	6.6	22.0
10/02 07:00:00	0.92	6.2	43.2	1.07	5.8	32.0
10/02 10:00:00	0.59	5.2	28.1	0.97	6.6	22.0
10/02 13:00:00	-0.15	6.1	359.2	0.88	6.6	34.0
10/02 16:00:00	0.04	5.7	26.3	0.75	6.6	16.0
10/02 19:00:00	0.66	3.9	44.2	0.63	6.2	30.0
10/02 22:00:00	0.41	1.9	96.3	0.57	7.0	18.0
10/03 01:00:00	-0.29	1.0	20.6	0.55	6.6	12.0
10/11 07:00:00	-0.06	9.5	22.5	1.09	4.8	36.0
10/11 0:00:00	-0.01	8.8	30.2	1.23	5.0	36.0
10/11 3:00:00	0.69	8.2	14.7	1.19	5.2	32.0
10/11 6:00:00	0.82	8.4	20.5	1.25	5.8	20.0
10/11 9:00:00	0.15	7.4	39.9	1.17	5.8	30.0
10/11 22:00:00	-0.11	6.1	45.7	1.16	10.7	-10.0
10/12 01:00:00	0.49	5.1	47.8	1.16	10.7	12.0
10/15 10:00:00	0.21	7.7	353.6	0.90	10.7	-16.0
10/15 13:00:00	-0.27	9.7	348.1	1.03	4.8	36.0
10/15 16:00:00	0.62	9.9	345.2	1.16	5.0	34.0
10/15 19:00:00	1.13	11.2	352.2	1.29	5.0	38.0
10/15 22:00:00	0.37	9.3	6.4	1.25	5.2	40.0
10/16 01:00:00	-0.25	7.2	360.0	1.18	5.2	42.0
10/16 04:00:00	0.56	7.2	324.1	1.24	10.7	-20.0
10/16 19:00:00	1.14	8.4	33.8	1.78	6.2	10.0
10/16 22:00:00	0.71	9.5	27.0	1.75	6.2	10.0
10/18 10:00:00	1.28	10.9	23.7	1.84	6.6	16.0
10/18 13:00:00	0.32	11.9	26.1	2.23	7.6	12.0
10/18 19:00:00	0.83	11.9	26.9	2.23	8.2	10.0

10/18 22:00:00	1.08	12.1	14.9	2.12	8.2	12.0
10/19 01:00:00	0.42	11.4	20.9	1.90	7.0	10.0
10/19 04:00:00	0.15	13.1	19.6	2.08	6.6	12.0
10/19 07:00:00	1.01	13.8	13.9	2.50	7.6	18.0
10/19 10:00:00	1.53	15.1	12.6	2.65	7.6	20.0
10/19 22:00:00	1.18	10.2	323.0	2.55	10.7	12.0
10/20 10:00:00	1.23	10.1	328.2	2.15	13.6	-6.0
10/20 13:00:00	0.85	9.7	327.8	1.98	13.6	-4.0
10/20 22:00:00	0.87	2.2	274.8	2.03	13.6	8.0

Chapter 3 2DH model of the SandyDuck97 cases

3.1 Introduction

The SandyDuck97 cases have been modelled with Delft3D-FLOW Version 3.55.05.779, Delft3D-WAVE Version 3.00.05.786 and SWAN (simulation of waves in nearshore areas) Version 40.51A. Appendix A and B contain the MDF-file (Master Definition Flow) and the MDW-file (Master Definition Wave) of the Delft3D model of the SandyDuck97 cases.

3.2 Computational grid

The rectangular flow grid has 86 cells in *M*-direction (cross-shore) and 117 in *N*-direction (longshore) with a grid spacing of 10 m in *M*- and 15 m in *N*-direction, which corresponds to a modelled area of 850 x 1740 m. The offshore boundary is at the 8 m directional wave gage array. The grid spacing of the wave grid is the same as of the flow grid, as well is the number of grid cells in *x*-direction. The number of cells in *y*-direction is larger (i146) to ensure realistic wave conditions of the cross-shore boundaries of the flow grid. A depth file was created for each day based on the available bathymetrical data.

3.3 Boundary conditions

At the longshore, Eastern boundary the water level is set to a constant value of zero meter. The vertical tide is taken into account by adjusting the depth files. Neumann boundaries are imposed at both cross-shore boundaries (Southern and Northern). The water level gradient is taken to be zero and constant in time and space. By doing this, the horizontal tide is neglected. Trial runs showed that including the horizontal tide has marginal effect on the cross- and longshore currents. At all wave boundaries a 2D (direction and frequency) wave spectrum is imposed based on the wave rider measurements at 8 m water depth.

3.4 Parameter settings

Table 3.1 shows the default Delft3D settings, the settings applied by Hsu et al. (2008) and the settings used in this study. Default settings are taken for the parameters not mentioned in this table.

Table 3.1 Parameters settings 2DH model of SandyDuck cases.

Parameter	Default D3D	Hsu et al.	Present
Simulation time (min)	-	60	60
Time step (min)	-	0.05	0.1
Reflection parameter alpha (s^{-2}) (for offshore water level boundary)	0	100	100
Water density (kg/m^3)	1000	1000	1025
Chézy roughness coefficient ($m^{0.5}/s$)	65	65	60
Background horizontal viscosity (m^2/s)	1	0	0
Threshold depth (m)	0.1	0.2	0.2
Smoothing time (min)	60	15	15
Interval wave computation (min)	-	30	30
Roller	no	yes	yes
Cstbnd	no	yes	yes
Gamdis	0.55	-1	-1

F_lam	0.0	0.0	0.0
Alfaro	1.0	1.0	1.0
Extend flow results on wave grid	yes	no	yes

The reflection parameter alpha makes the open offshore water level boundary less reflective for disturbances that occur at the start of the computation. By setting alpha to 100 (a typical value), the initial disturbances propagate out of the model quickly and the spin-up time for the hydrodynamics is relatively short.

The threshold depth is the depth above which a grid cell is considered to be wet. The threshold depth must be defined in relation to the change of the water depth per time step in order to prevent the water depth to become negative in just one time step. This would result in iterations in the computation and thus a larger computational time. Based on this consideration, a threshold depth of 0.1 m would be more than sufficient for the SandyDuck97 cases since we impose a constant water level at the offshore boundary, and the change in set-down/set-up (driven by radiation stress) will be marginal. However, the threshold depth also affects the currents since the roller stress is turned off at a twice the threshold depth. Hsu et al. (2006) showed that the roller stress should be turned off at shallow depth (0.4 m, corresponding to a threshold depth of 0.2 m) to avoid spuriously high currents.

The smoothing time is the time interval used at the start of a simulation for a smooth transition between initial and boundary conditions. In some cases, the prescribed initial condition and the boundary values at the start time of the simulation do not match. This can introduce large spurious waves that enter the model area that reflect at the boundaries until the wave energy is dissipated. This enhances the spin-up time of the model. To reduce this time, a smooth transition period can be specified, during which the boundary condition will be adapted gradually starting from the prescribed initial condition value. Since the offshore water level boundary matches the initial water level (both equal zero), a smoothing time of 15 minutes is sufficient for the SandyDuck cases.

Wave heights are computed using the roller model (see Reniers et al, 2004). The roller model consists of balance equations for the short wave energy and the roller energy. Wave energy dissipation due to wave breaking is a sink term in the first equation and acts as a source term for the roller energy equation, reflecting the conversion of organised wave energy to turbulent kinetic energy in the form of a roller at the face of a breaking wave. The roller energy equation is closed by including dissipation of roller energy as a sink term. In this way the region of wave-set up is shifted in shoreward direction as well as the wave-driven currents. The roller model uses the peak frequency and mean wave direction as computed by SWAN as input. Hsu et al. (2006) showed that the roller model improved the current prediction.

By putting the keyword “Cstbnd” to “yes” the advection terms at the offshore boundary containing normal gradients are switched off to avoid the generation of an artificial boundary layer along the boundary.

γ determines the maximum wave height that can occur at a given depth. A constant γ can be selected or the expression of Ruessink et al. (2003) can be used where γ is a function of the wave length (inversely proportional) and the water depth (proportional) (in shallow water $\gamma \sim h^{0.5}$). Compared to a typical fixed γ-value (0.5-0.8), the variable gamma leads to higher waves in deeper water and lower waves in more shallow water.

Hsu et al. (2006,2008) showed that the γ-expression of Ruessink et al. improved wave height prediction.

Based on trial runs for SandyDuck cases 97101513 and 97101916, a “normal” event with H_s = 1.0 m and a storm event with H_s = 3.5 m, two parameter settings were changed compared to Hsu et al’s settings.

- Time step of 0.1 min instead of 0.05 min. By doing this, the computational time is reduced, while computed wave heights and currents are hardly affected.
- Extension of the water levels, currents and wind on the wave grid in areas that are not covered by the flow grid. In this way, a more uniform wave field is computed at the boundaries of the flow grid.

Furthermore, a water density of 1025 kg/m^3 is taken instead of 1000 kg/m^3 since this is a more realistic value for salt water.

3.5 Sensitivity runs

In this section we will test the sensitivity of the model predictions of the wave heights and longshore current velocities to the Chézy roughness coefficient *C*, the background horizontal viscosity $\nu_{h,back}$, α (breaker coefficient) and inclusion of breaker delay. The results are presented in Figure 3.1 to Figure 3.12. These include both comparison between all measured and predicted data points, as well as a sample comparison between measured and computed wave heights and longshore current velocities as a function of the cross-shore distance (SandyDuck case 97101513). We define cross-shore current *U* to be positive in onshore (Western) direction, and longshore current *V* to be positive in Northern direction.

As can be seen in Figure 2.2, certain wave height measurements were carried out relatively close to each other, i.e. at $x \approx$ 210, 260, 380 and 500 m. To avoid the assessment of the model performance to be biased to these locations, wave height measurements at these locations are averaged (as well are the *x*- and *y*-coordinates). This results in a data-model comparison on the basis of 18 instead of 27 wave height measurement locations. It was not necessary to make this correction for the current measurements, as the inner spacing between measurement locations was larger.

The goodness of fit is quantified through the mean and the standard deviation of the relative error:

$$\bar{\mu} = \frac{1}{N}\sum_i^N \mu_i = \frac{1}{N}\sum_i^N \frac{C_i - M_i}{M_i} \quad (1)$$

$$\sigma = \sqrt{\frac{1}{N}\sum_i^N \left(\mu_i - \bar{\mu}\right)^2} \quad (2)$$

with M_i and C_i represent measured and computed quantities. If $\bar{\mu} > 0$ the measurements are overpredicted on average; the measurements are underpredicted if $\bar{\mu} < 0$. $\sigma = 0$ means that there is no deviation in the individual computed parameters; the larger σ, the larger the deviation in the computations.

Figure 3.1 and Figure 3.2 show that the Chézy roughness coefficient has virtually no effect on the computed wave heights. This is because the wave dissipation due to bottom friction is not taken into account in the balance equation for short wave energy. Including the effect of bottom friction on the wave height would probably not have a large effect for the present cases, since wave computations are made over a relatively short distance and most measurements were carried out in the surf zone where dissipation due to wave breaking is dominant. However, the absence of dissipation due to bottom friction could explain the general overprediction of wave heights. It is recommended to include this sink term in the roller model. The *C*-value has quite a strong effect on the computed longshore velocities. An decrease in *C* (increasing roughness) leads to a higher bed shear stress and a reduction in current velocities. Best agreement is obtained with $C = 60\ m^{0.5}/s$.

The background horizontal viscosity has no (direct) effect on the wave height calculations. However, it has a quite strong impact on the computed velocities. An increase in $v_{h,back}$ increases the horizontal momentum exchange. As a result, the currents are spread out more uniformly. Closest agreement between measured and modelled longshore current velocities is achieved by taking $v_{h,back} = 0.0\ m^2/s$.

Breaker delay can be regarded as an extension to the roller model. The breaker delay parameter “”F_lam” is set to -2, which means that energy dissipation due to wave breaking is computed using a water depth that follows from a weighted average from the local water depth up to the water depth two wave lengths offshore. Since the water depth generally increases in offshore direction, including breaker delay delays the energy dissipation due to wave breaking and consequently wave heights are higher. According to Walstra (2000), including breaker delay generally improves wave height predictions in case of swell-type of conditions, but in case of short waves it often leads to an overprediction of the wave heights. The latter is the case for the SandyDuck cases. Including breaker delay generally moves peak (wave-driven) longshore velocities in onshore direction (not shown here). Seaward of this point longshore currents are generally weaker than without breaker delay; shoreward longshore current are generally stronger. This results in a better prediction of the longshore currents, but since wave height predictions worsened and the systematic overprediction of the currents will be improved by lowering the Chézy coefficient, we chose not to include breaker delay in the further calculations.

Figure 3.10, Figure 3.11 and Figure 3.12 show the effect of α on the wave height and longshore current predictions. α is a coefficient in the expression for the dissipation due to wave breaking; this dissipation term is proportional to α. According to Walstra (2000), α should be in the range 0.6-1.2. An increase in α results in a decrease of the wave height in the surf zone where wave breaking is important, as can be seen, although the effect is not so strong. The wave height is slightly better predicted for the larger value of α, but since the computed current velocities agree worse with the measurements, we stick to the original (default) value of the wave breaking coefficient.

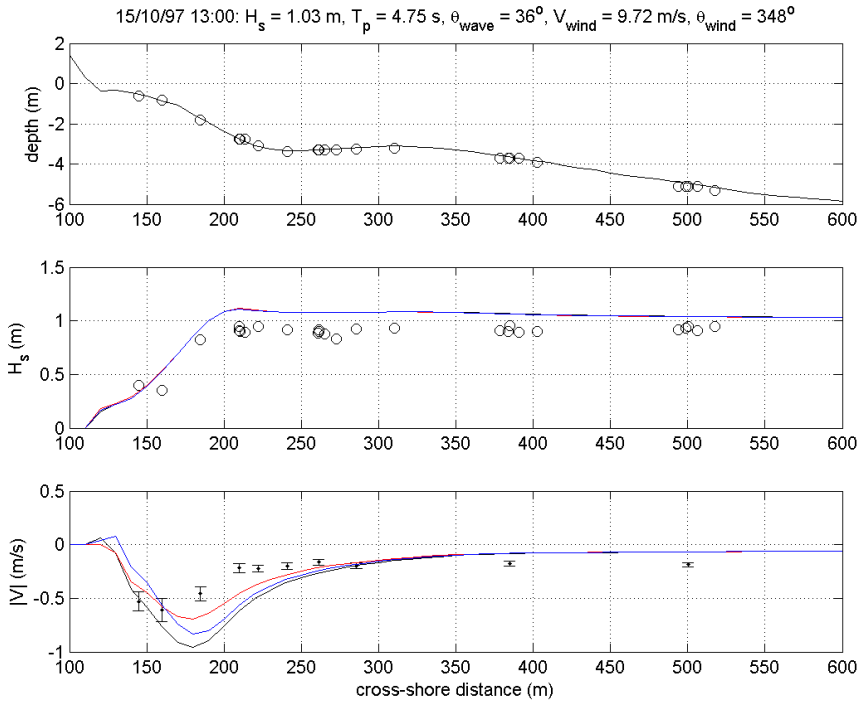

Figure 3.1 *Comparison between measured and computed wave heights and longshore currents as function of the cross-shore distance for different Chézy roughness coefficients C. Black lines: C = 65 $m^{0.5}$/s (default value); red lines: C = 55 $m^{0.5}$/s; blue lines: C = 60 $m^{0.5}$/s.*

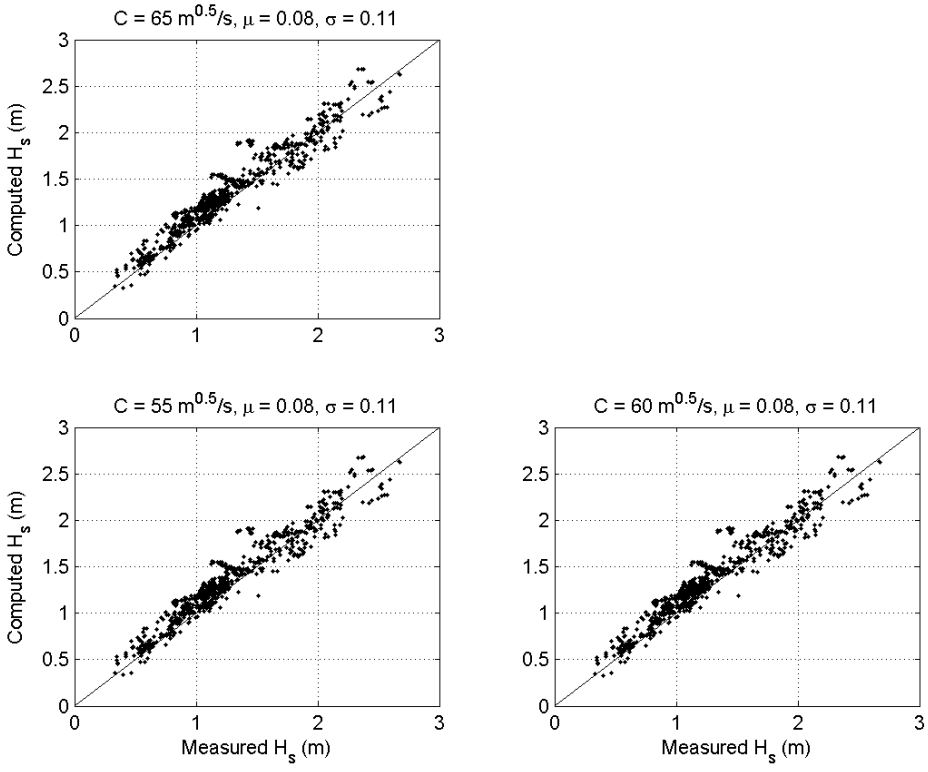

Figure 3.2 *Comparison between measured and computed wave heights for different Chézy roughness coefficients C.*

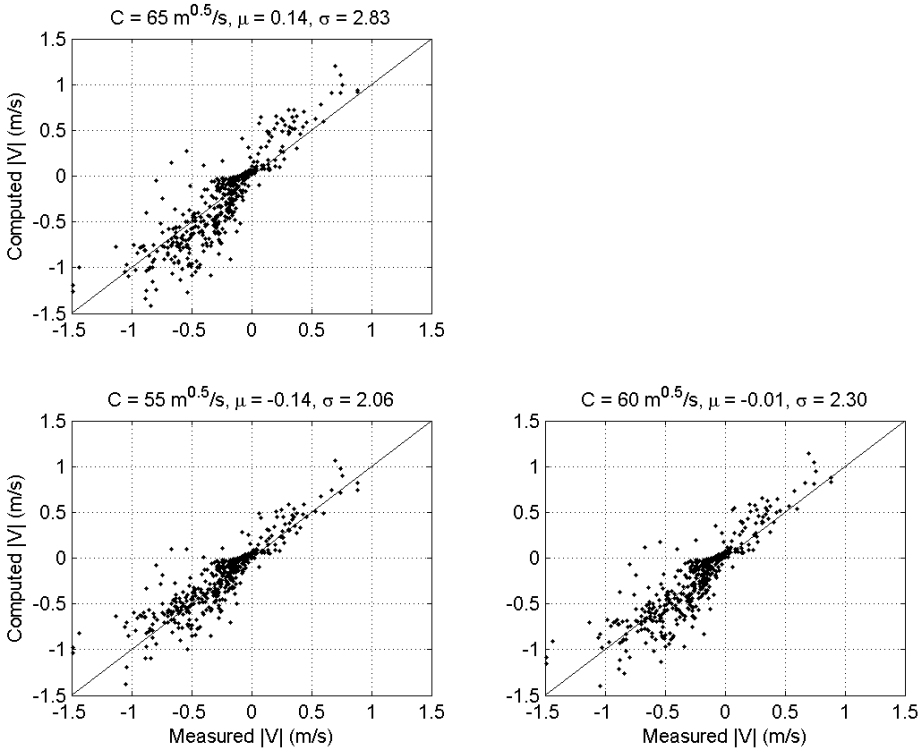

Figure 3.3 *Comparison between measured and computed longshore currents for different Chézy roughness coefficients C.*

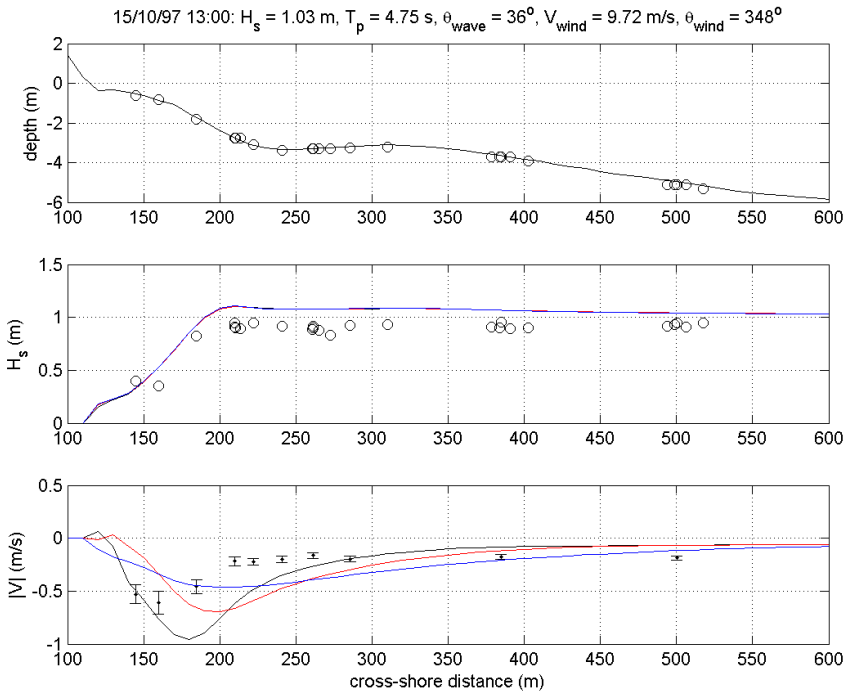

Figure 3.4 *Comparison between measured and computed wave heights and longshore currents as function of the cross-shore distance for different values of the horizontal background viscosity $\nu_{h,back}$. Black lines: $\nu_{h,back}$ = 0.0 m^2/s (default value); red lines: $\nu_{h,back}$ = 1.0 m^2/s; blue lines: $\nu_{h,back}$ = 5.0 m^2/s.*

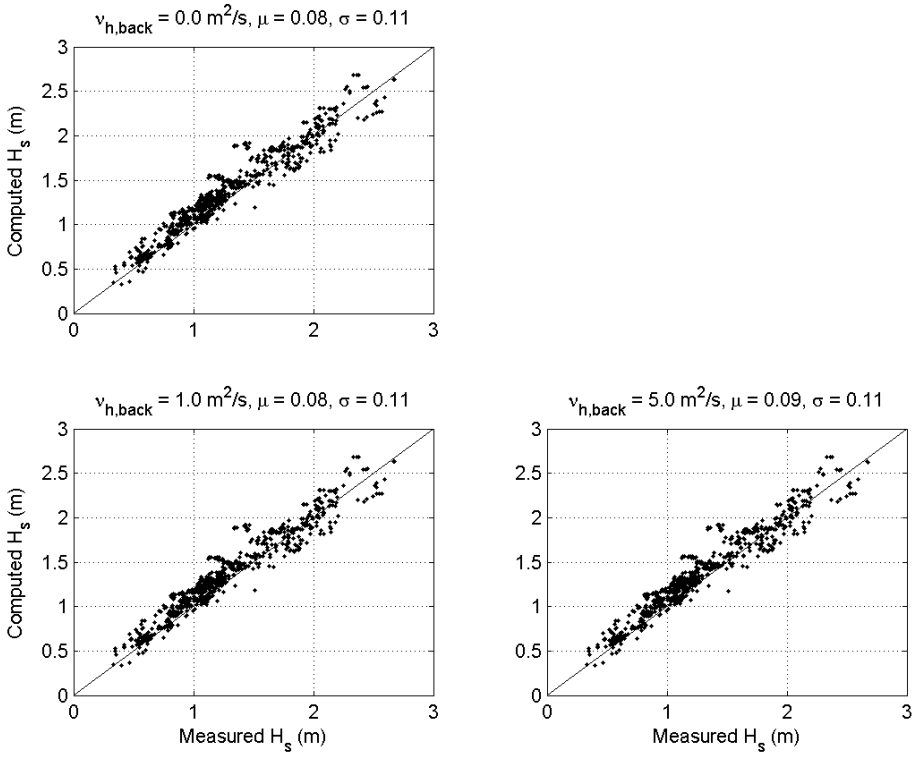

Figure 3.5 Comparison between measured and computed significant wave heights for different values of the horizontal background viscosity $\nu_{h,back}$.

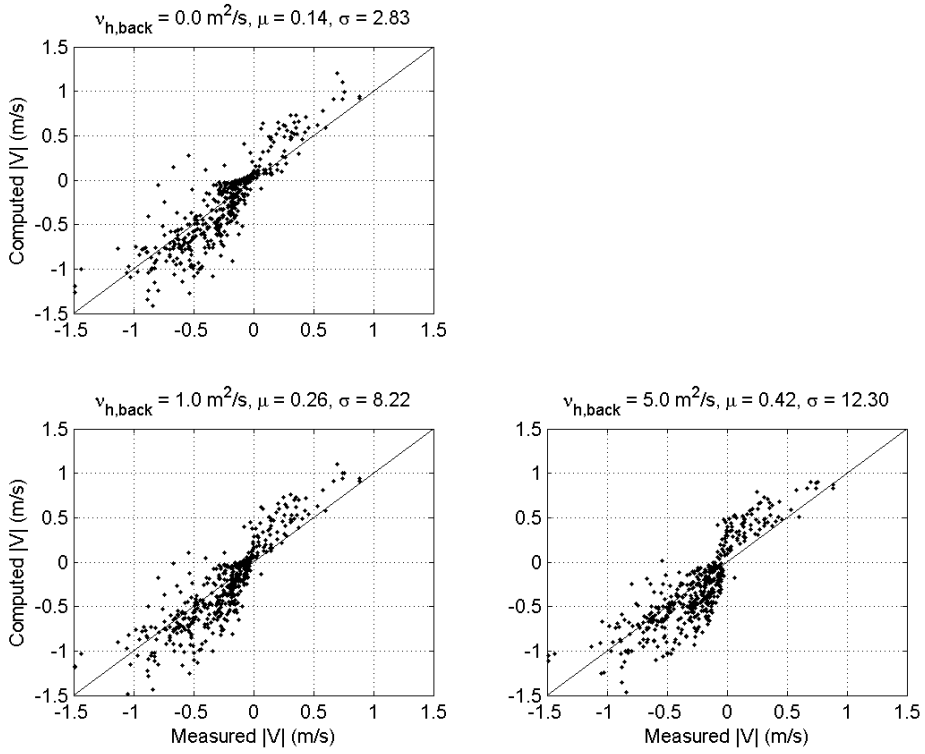

Figure 3.6 Comparison between measured and computed longshore current velocities for different values of the horizontal background viscosity $\nu_{h,back}$.

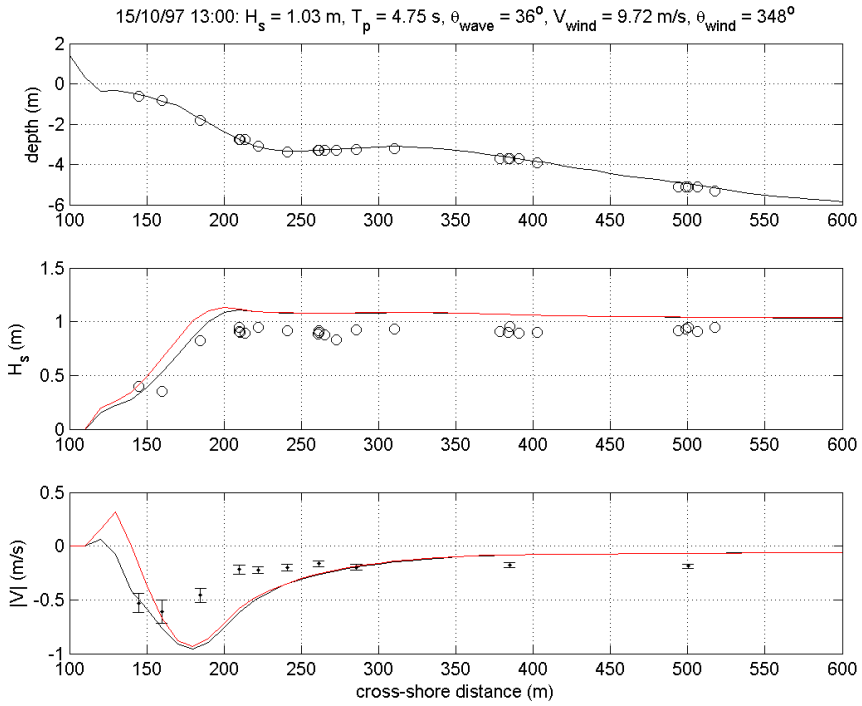

Figure 3.7 *Comparison between measured and computed wave heights and longshore currents as function of the cross-shore distance. Black lines: without breaker delay (default value); red lines: with breaker delay.*

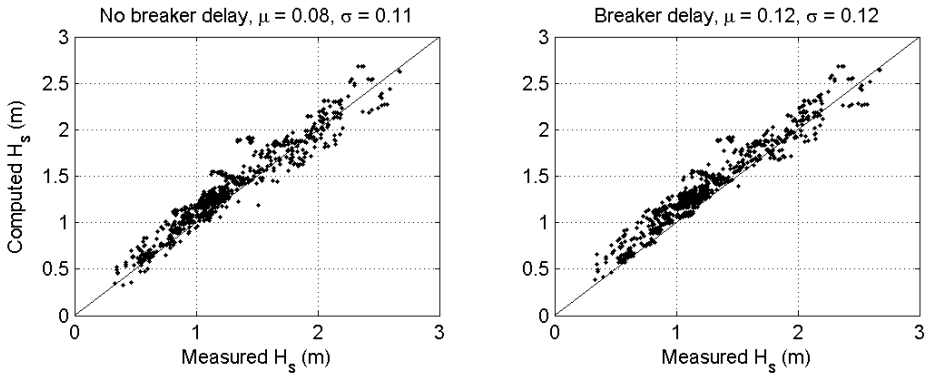

Figure 3.8 *Comparison between measured and computed significant wave heights with and without breaker delay.*

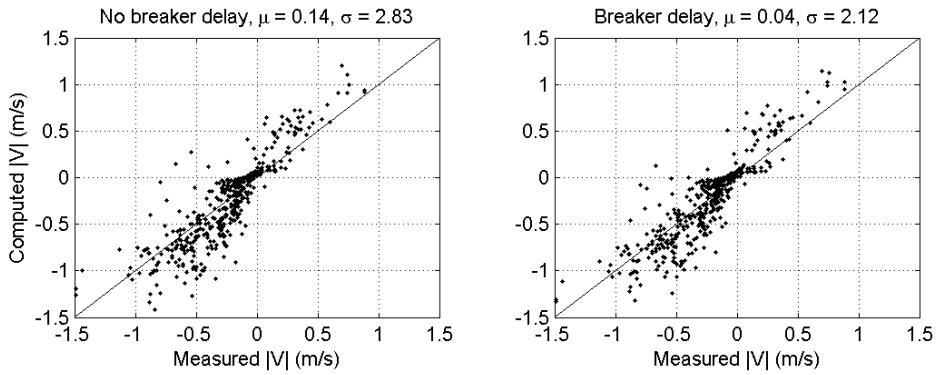

Figure 3.9 *Comparison between measured and computed longshore current velocities with and without breaker delay.*

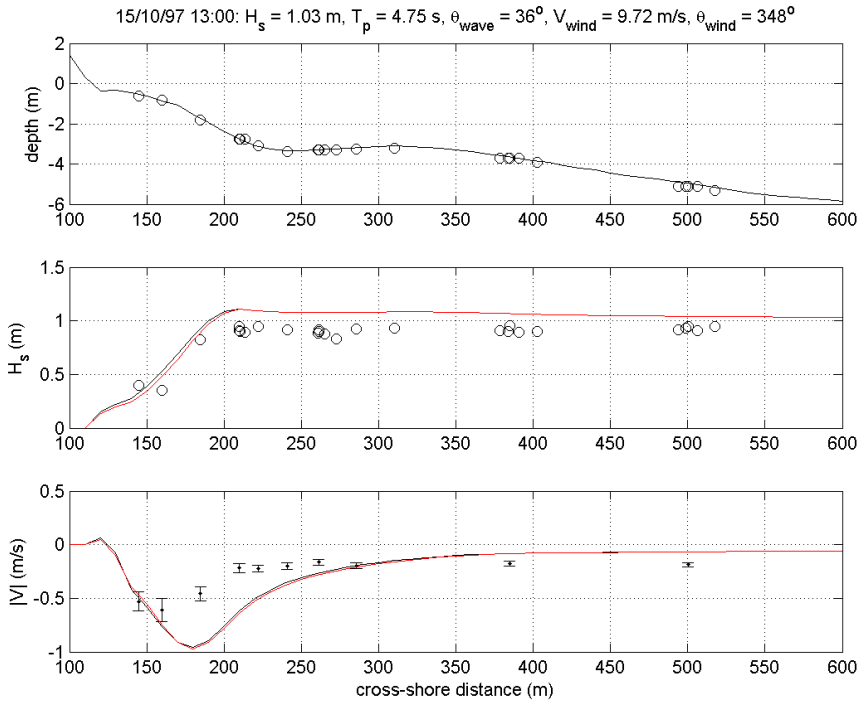

Figure 3.10 *Comparison between measured and computed wave heights and longshore currents as function of the cross-shore distance for different values of wave breaking coefficient α. Black lines: α = 1 (default value); red lines: α = 1.2.*

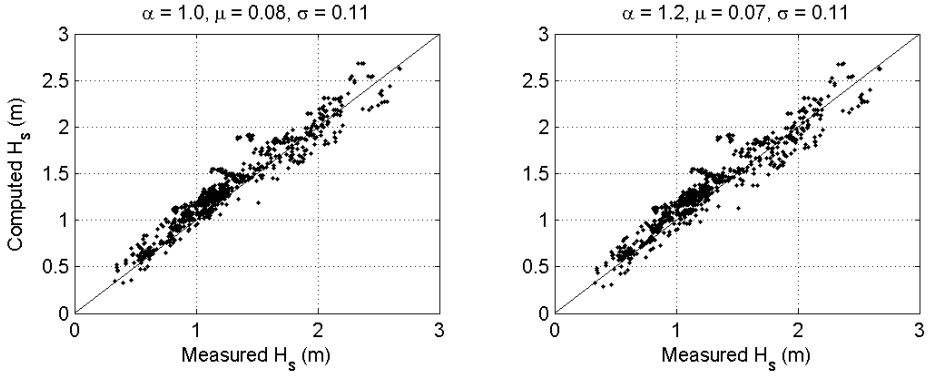

Figure 3.11 *Comparison between measured and computed wave heights for different values of wave breaking coefficient α.*

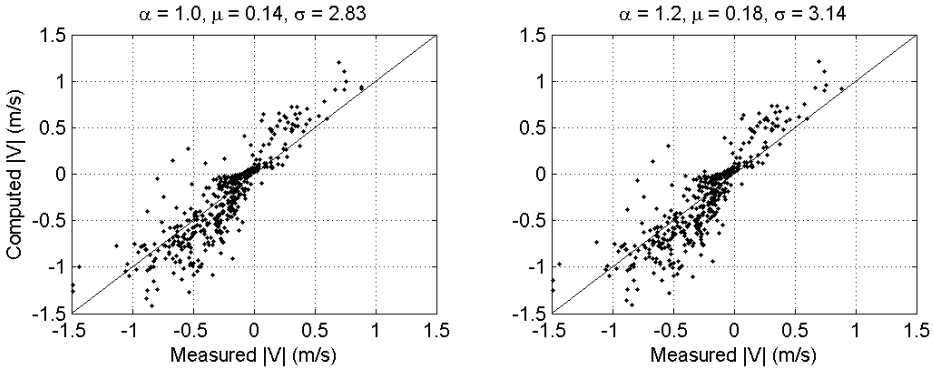

Figure 3.12 Comparison between measured and computed longshore current velocities for different values of wave breaking coefficient α.

3.6 Assessment capability 2DH model to predict nearshore wave and flow field

The 2DH model with the settings as given in Table 3.1 overpredicts the wave height on average with 8% with a standard deviation of 11%. Figure 3.13 shows that the wave height is overpredicted with more a less the same amount along the cross-shore transect, which could be related to the absence of wave dissipation due to bottom friction. The spreading in the relative error in the wave height computations tend to increase in shoreward direction.

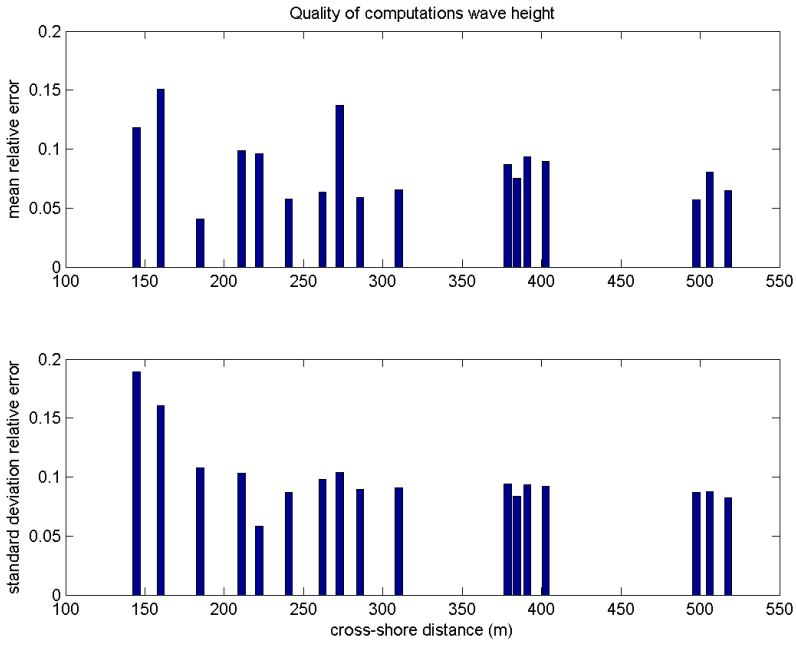

Figure 3.13 The mean relative error and the standard deviation of the relative error as function of the cross-shore distance for the 2DH wave height computations.

The longshore currents are on average neither under- nor overpredicted, but the standard deviation of the relative error is rather large, which can clearly be seen in Figure 3.14. In general, the 2DH model underpredicts the longshore currents offshore (x > 250 m) and overpredicts closer to the shore. (Note that under- and overprediction refer to the magnitudes of the currents not to the directions!). It can be observed that at

$x \approx$ 241 m the current velocities are underpredicted on the average, while at the neighbouring measurement locations velocities are overpredicted. The standard deviation of the relative error as well as the variance in the measurements are largest between x = 200 and 250 m, which corresponds to the location where for most of the cases the peak in longshore current occurs. On average the model computations are within the variance of the measurements.

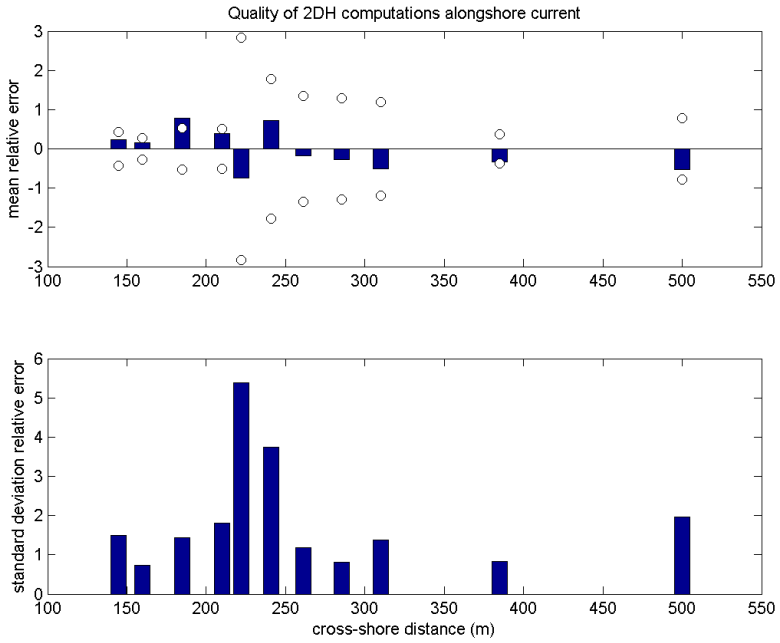

Figure 3.14 The mean relative error and the standard deviation of the relative error as function of the cross-shore distance for the 2DH longshore current computations. The open circles indicate the variance in the measurements.

Figure 3.15 shows that the cross-shore locations of the longshore velocity maxima are in general underpredicted. This means that the computed peak in the longshore current is too far onshore compared to the measurement. At the same time, the magnitude of this longshore current maximum is overpredicted by the model, which could be related to the overprediction of the wave height.

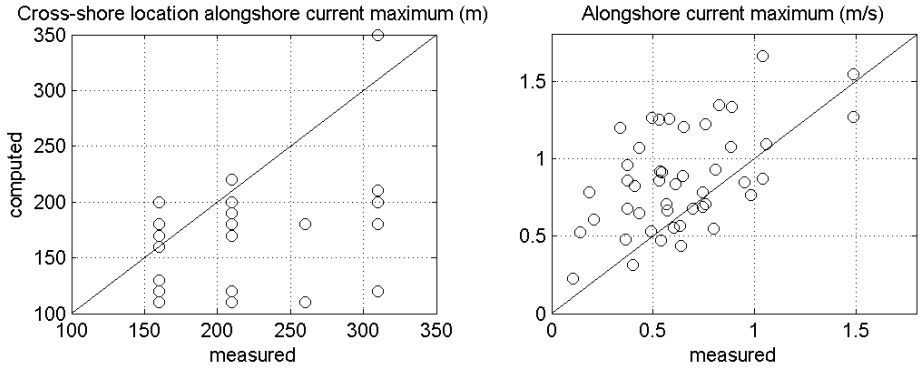

Figure 3.15 Comparison between measured and computed cross-shore location and magnitude of the longshore current maximum.

We have also investigated the relation between the wind and wave conditions on the capability of the 2DH model to predict wave heights and longshore current velocities. This analysis showed that i) high waves have in general a more shore normal direction than low waves, ii) the model tends to overpredict the wave height for low wave events and underpredict for high wave events, iii) both wave heights and longshore currents are better predicted for high wave events.

Chapter 4 3D model of the SandyDuck97 cases

4.1 Model settings

We use the same model settings as for the 2DH model, see Table 3.1. As a default, we take the *k*-ε turbulence model and divide the water column in 20 layers with from the surface to the bed the following distribution: 0.7%, 1.0%, 1.4%, 2.0%, 2.8%, 3.9%, 5.4%, 7.5%, 10.6%, 14.7%, 14.7%, 10.6%, 7.5%, 5.4%, 3.9%, 2.8%, 2.0%, 1.4%, 1.0%, 0.7%. Thus thin layers near the bed and surface and thicker layers in the middle of the water column. This fining is necessary to take good account of the driving forces near the bed (bottom friction, stress to model Longuet-Higgins streaming) and near the surface (wind- and wave-induced forcing), and of the wave-induced turbulent kinetic energy (both near the surface and the bed).

Below we study the effect of the turbulence model (*k*-ε and *k*-*L*) and the number of layers (10, 20, 30, 40, 50) on the longshore current computations with the measurements as a reference. Then we compare the 3D model with the measurements and the 2DH model.

4.2 Effect of the turbulence model

The *k*-*L* turbulence model is a so-called first-order turbulence closure scheme. The turbulent kinetic energy *k* follows from a transport equation that includes an energy dissipation term, a buoyancy term and a production term. The dissipation term is related to the mixing length *L*, which is prescribed analytically. The eddy viscosity is proportional to the mixing length and the square root of the turbulent kinetic energy.

In the *k*-ε turbulence model the same transport equation for the turbulent kinetic energy is solved as in the *k*-*L* turbulence model, but now also a transport equation is solved for the turbulent kinetic energy dissipation ε. This equation contains production, buoyancy and dissipation terms. The eddy viscosity is proportional to k^2/ε or, equivalent to the *k*-*L* model, $k^{0.5}L$.

The vertical mixing is enhanced by the wave action. Due to wave breaking, white-capping and bottom friction in the wave boundary layer wave energy is transferred to turbulent kinetic energy. This is accounted for by adding source terms in the *k*- and ε-model.

According to Savioli (2000), the *k*-*L* turbulence model is sufficient for cases where the effects of advection and diffusion of the turbulent length-scale are not significant, as in the *k*-*L* model *L* is locally determined. However, in re-circulating or rapidly changing flows a transport equation for the length scale is required to have a more physically realistic description.

Figure 4.1 to Figure 4.4 show vertical profiles of the longshore current velocity and of the eddy viscosity at four cross-shore locations for two cases: 97101201 and 97101922. Conditions were:

- 97101201 case: V_{wind} = 5.1 m/s, $\theta_{wind} = 48^o$, H_s = 1.2 m, $\theta_{Tp} = 12^o$, T_p = 10.7 s,
- 97101922 case: V_{wind} = 10.2 m/s, $\theta_{wind} = 323^o$, H_s = 2.6 m, $\theta_{Tp} = 12^o$, T_p = 10.7 s

The figures also include the measured velocity.

4.2.1 The 97101201 case

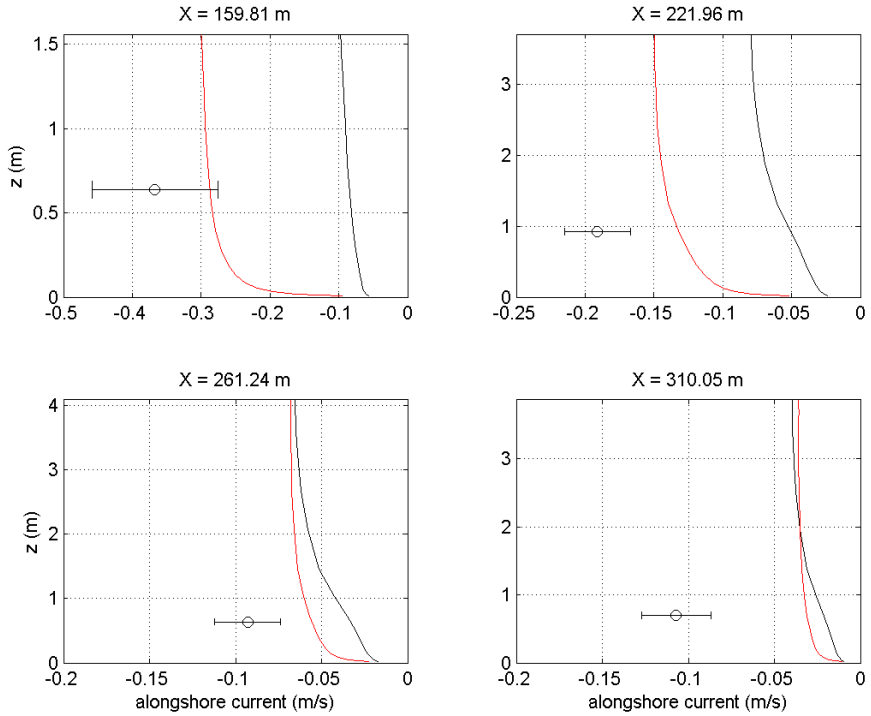

Figure 4.1 *Vertical profiles of the longshore current velocity at four cross-shore locations for SandyDuck case 97101201. Open circles: measured, black lines: computed using the k-ε turbulence model, red lines: computed using the k-L turbulence model.*

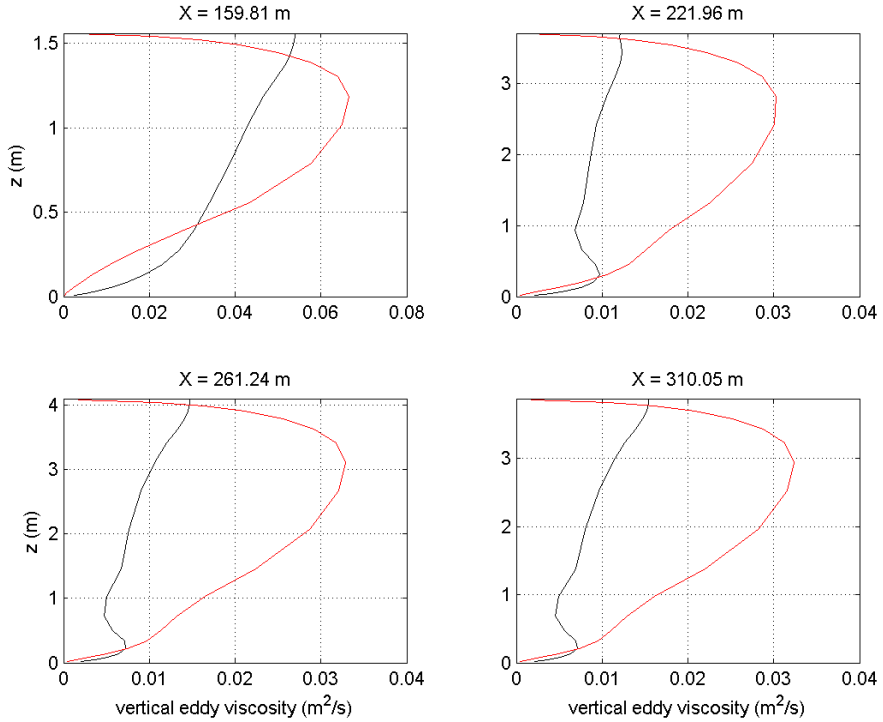

Figure 4.2 *Vertical profiles of the vertical eddy viscosity at four cross-shore locations for SandyDuck case 97101201. Black lines: computed using the k-ε turbulence model, red lines: computed using the k-L turbulence model.*

4.2.2 The 97101922 case

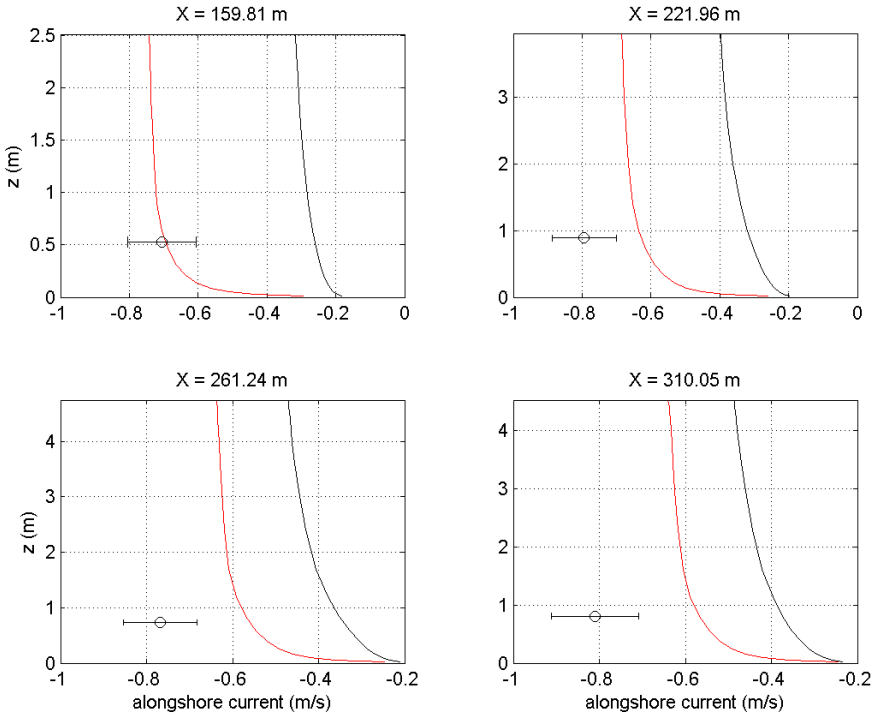

Figure 4.3 *Vertical profiles of the longshore current velocity at four cross-shore locations for SandyDuck case 97101922. Open circles: measured, black lines: computed using the k-ε turbulence model, red lines: computed using the k-L turbulence model.*

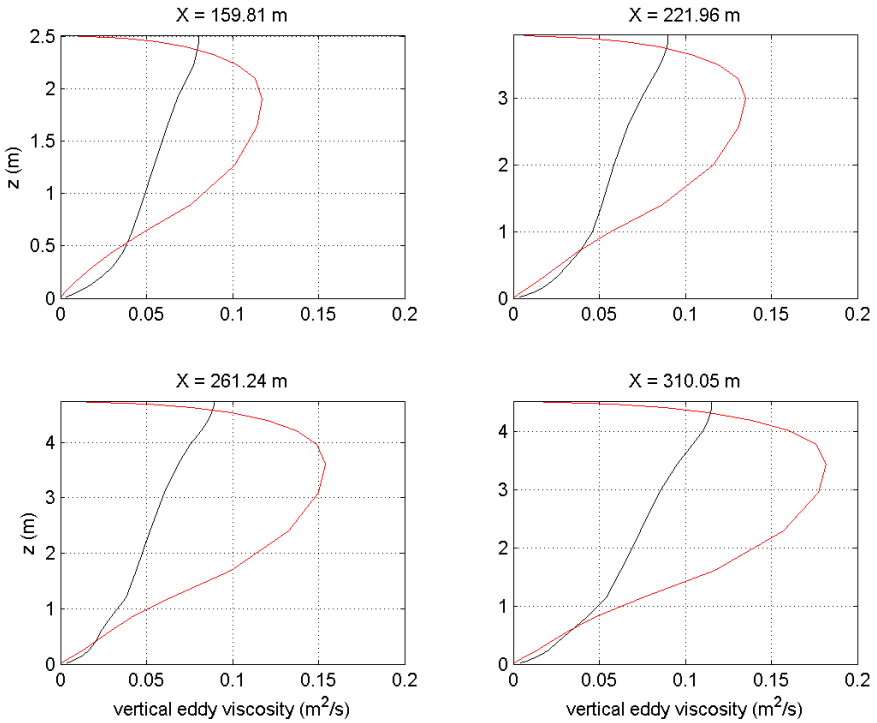

Figure 4.4 *Vertical profiles of the vertical eddy viscosity at 4 cross-shore locations for SandyDuck case 97101922. Black lines: computed using the k-ε turbulence model, red lines: computed using the k-L turbulence model.*

These figures show that there can be quite large differences between the model results obtained with the two different turbulence models. The longshore current velocities predicted with the *k*-*L* turbulence model are generally higher (not only for the two cases shown below), which is, at least partly, related to the difference in the vertical eddy viscosity profiles. Due to the algebraic formulation used to predict the turbulent length scale *L* the vertical eddy viscosity predicted by the *k*-*L* turbulence model has a parabolic shape with a zero eddy viscosity at the bed and at the surface and a maximum near $z = 5/8H$. The vertical eddy viscosity profile given by the *k*-ε turbulence model is more uniformly distributed over the water column because of diffusion and advection of the turbulent length scale. As a result of this, the eddy viscosity according to the *k*-ε turbulence model is larger both near the bed and the water surface. Therefore, the velocity gradient near the bed is smaller resulting in lower near-bed velocities and, as shear is decreasing with distance from the bed, the depth-averaged currents are lower as well for the *k*-ε turbulence model.

4.3 Effect of the number of vertical computational layers

Figure 4.5 to Figure 4.8 show the effect of the number of computational layers on the vertical profiles of the longshore currents and vertical eddy viscosity at four cross-shore locations for the cases 97101201 and 97101922. We use the *k*-ε turbulence model and vary the number of layers between 10 and 50. The layer distribution corresponding to the number of layers is controlled by 1) the choice for a logarithmic distribution with thinner layers both near the surface and the bed, 2) the factor by which a layer is allowed to differ from his neighbouring layers (1.4), 3) the minimal layer thickness (0.1%). The resulting layer distributions are (only the five top and bottom layer thicknesses):

- 10 layers: 4.6%, 6.4%, 9.0%, 12.5%, 17.5%, 17.5%, 12.5%, 9.0%, 6.4%, 4.6%
- 20 layers: 0.7%, 1.0%, 1.4%, 2.0%, 2.8%, … , 2.8%, 2.0%, 1.4%, 1.0%, 0.7% (default)
- 30 layers: 0.1%, 0.2%, 0.3%, 0.4%, 0.5%, … , 0.5%, 0.4%, 0.3%, 0.2%, 0.1%
- 40 layers: 0.1%, 0.1%, 0.1%, 0.1%, 0.1%, … , 0.1%, 0.1%, 0.1%, 0.1%, 0.1%
- 50 layers: 0.1%, 0.1%, 0.1%, 0.1%, 0.1%, … , 0.1%, 0.1%, 0.1%, 0.1%, 0.1%

These figures show that there appears to be a correlation between the number of vertical layers and the predicted vertical profile of the longshore current. The larger the number of layers, the smaller the predicted current velocities. This can especially be observed if the number of layers increases from 10 to 20. It does not make a large difference whether the number of layers is either 30, 40 or 50. It seems as if the controlling factor is the thickness of the bottom (and possibly the surface) computational layer, which is confirmed by the study of Treffers (in preparation). This dependency on the lower layer thickness can be explained as follows.

Delft3D computes the bed shear stress using the velocity in the lowest computational layer and a Chézy roughness coefficient that follows from the assumption that the current distribution is logarithmic in this layer. This means that this Chézy roughness coefficient decreases with the thickness of the lowest computational layer (or: the bed is “rougher”). If the velocity profile is logarithmic, this results in the same bed shear stress regardless of the layer thickness. In case the velocity profile is more uniformly

distributed near the bed, e.g. due to the action of waves, then a thinner layer gives a relatively "rougher" bed and the current is slowed down.

4.3.1 The 97101201 case

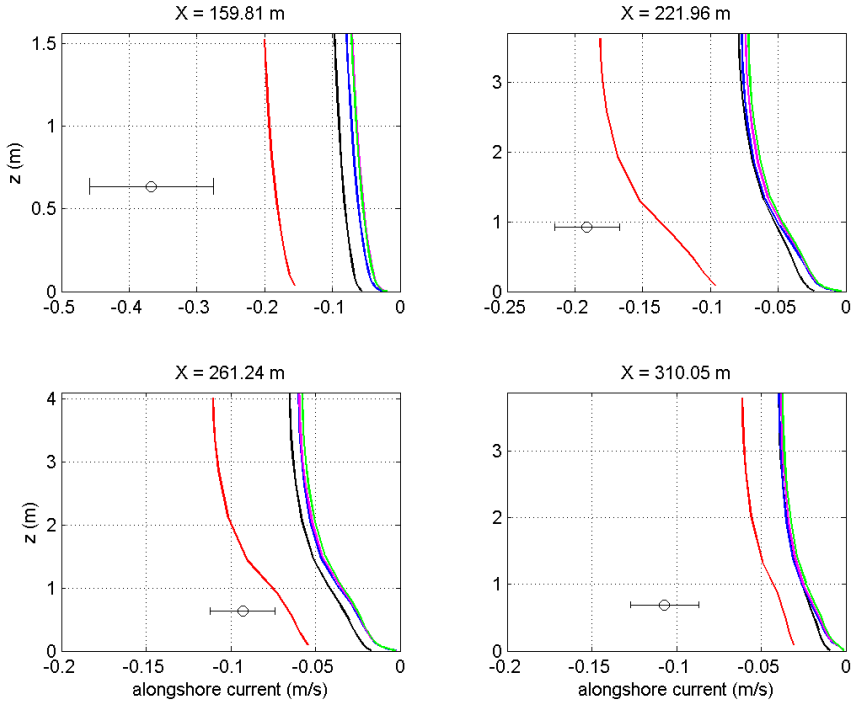

Figure 4.5 *Vertical profiles of the longshore current velocity at four cross-shore locations for SandyDuck case 97101201. Open circles: measured, black lines: 20 vertical layers (default), red lines: 10 vertical layers, blue lines: 30 vertical layers, magenta lines: 40 vertical layers, green lines: 50 vertical layers.*

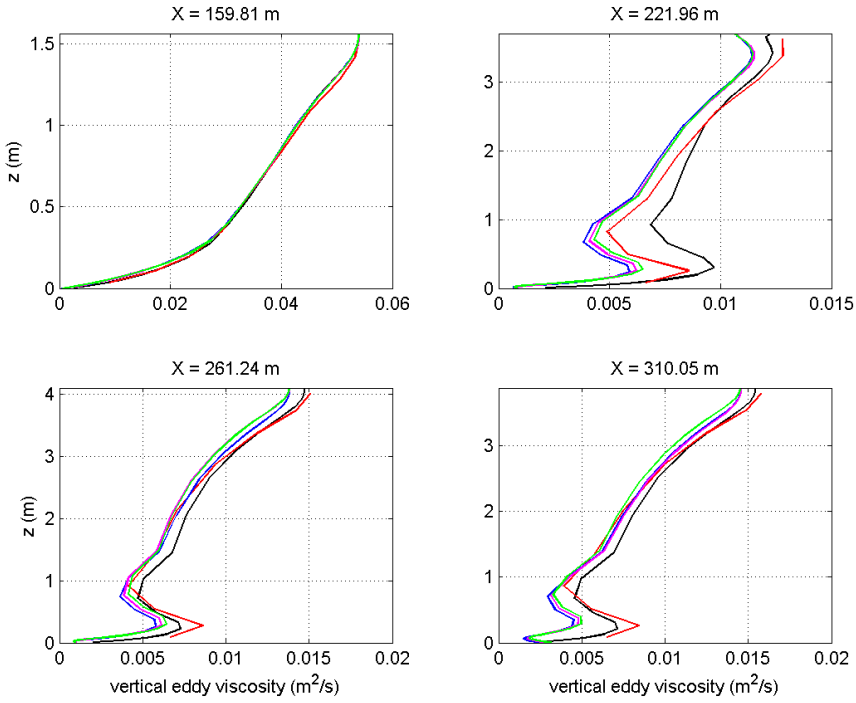

Figure 4.6 *Vertical profiles of the vertical eddy viscosity at four cross-shore locations for SandyDuck case 97101201. Open circles: measured, black lines: 20 vertical layers (default), red lines: 10 vertical layers, blue lines: 30 vertical layers, magenta lines: 40 vertical layers, green lines: 50 vertical layers.*

4.3.2 The 97101922 case

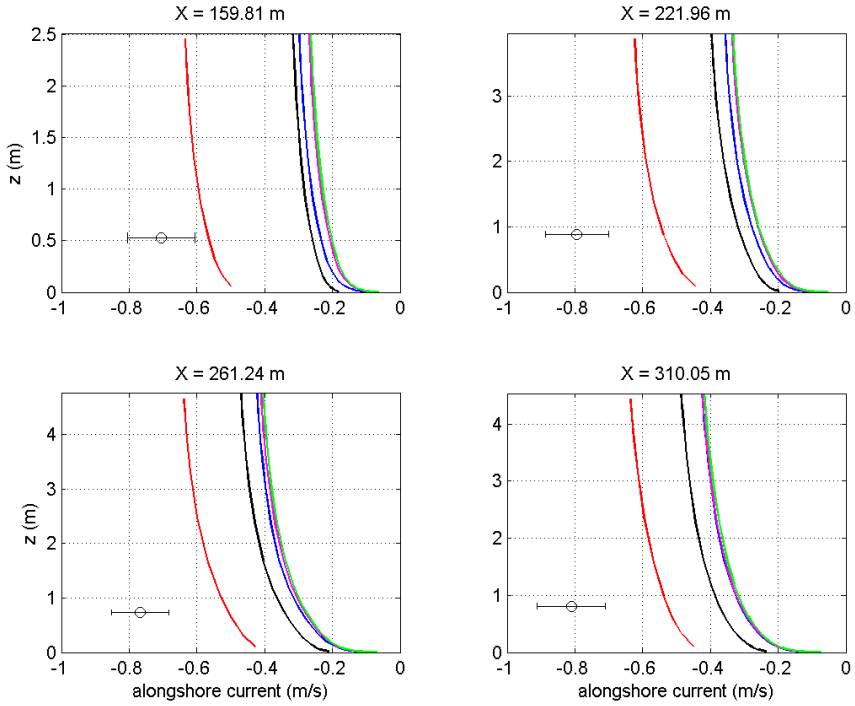

Figure 4.7 *Vertical profiles of the longshore current velocity at four cross-shore locations for SandyDuck case 97101922. Open circles: measured, black lines: 20 vertical layers (default), red lines: 10 vertical layers, blue lines: 30 vertical layers, magenta lines: 40 vertical layers, green lines: 50 vertical layers.*

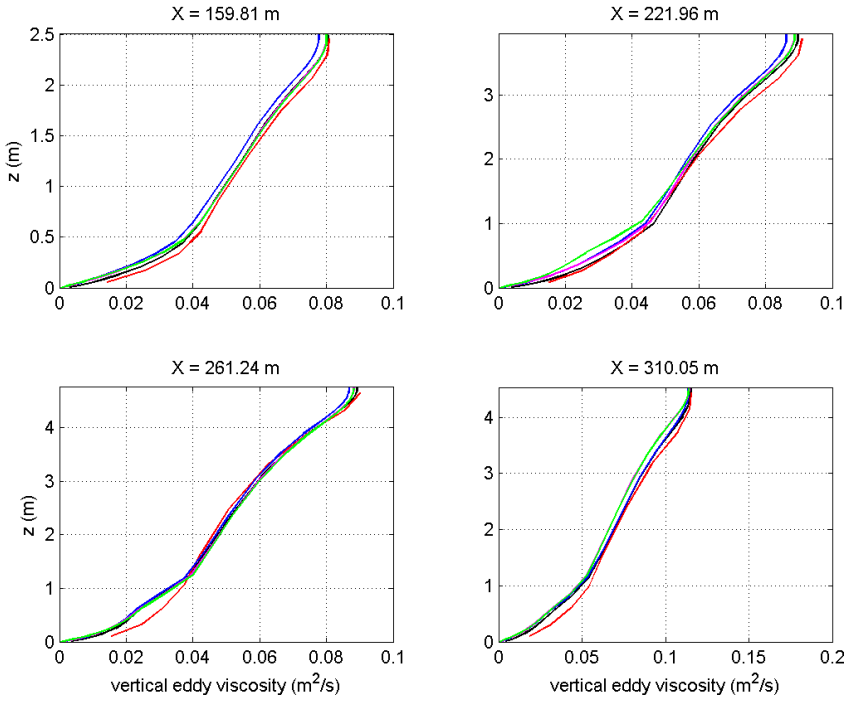

Figure 4.8 *Vertical profiles of the vertical eddy viscosity at four cross-shore locations for SandyDuck case 97101922. Open circles: measured, black lines: 20 vertical layers (default), red lines: 10 vertical layers, blue lines: 30 vertical layers, magenta lines: 40 vertical layers, green lines: 50 vertical layers.*

In general, the vertical eddy viscosity are not too much affected by the number of computational layers, except for locations where wave energy dissipation due to wave breaking and bottom friction are large. These source terms for the turbulence model are linearly distributed over half a wave height below the mean water surface and over the thickness of the wave boundary layer, respectively. Then it matters whether the centre of the computational layers are located in this region or not.

4.4 Comparisons between the 2DH and 3D model

Figure 4.9 compares the depth-averaged longshore current velocities at all (11) measurement locations predicted by the 2DH and the 3D model for all 46 SandyDuck cases. Comparison is made for the 3D model with 20 vertical layers (black dots) and 10 vertical layers (red dots). This figure shows that the depth-averaged currents computed by the 3D model are consistently lower than those computed by the 2DH model. Furthermore, the ratio between the depth-averaged currents predicted by the 2DH and 3D model is proportional to the number of vertical layers (or the thickness of the bottom computation layer), which confirms the findings from Section 4.3 . For 10 vertical layers, the longshore currents computed the 3D model are on average 11% lower; for 20 vertical layers on average 39%.

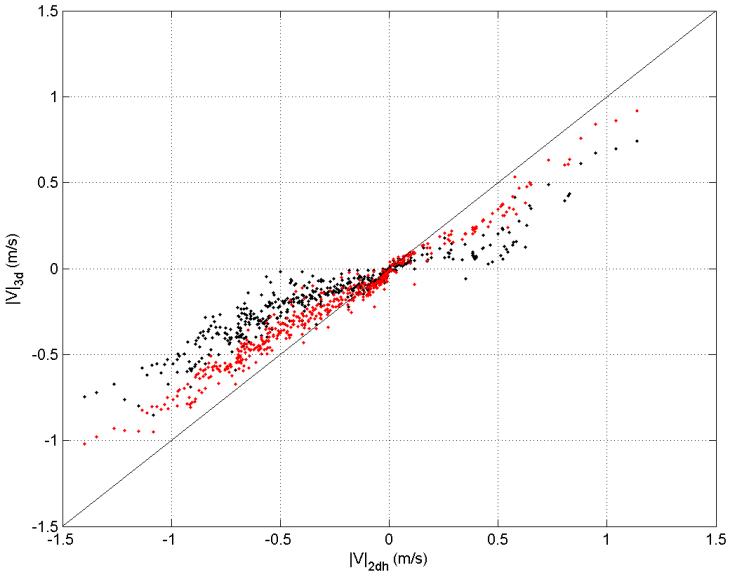

Figure 4.9 Comparison between depth-averaged longshore current velocities computed by the 2DH and the 3D model. Black dots: 20 layer 3D model, red dots: 10 layer 3D model.

This difference has already been noticed by Luijendijk (2007). He studied the difference by omitting all relevant 3D processes and then step-by-step re-including these processes to assess the impact of individual processes for idealized cases. He concluded that the *k*-ε turbulence model, including cross-shore velocities in the bed shear stress calculation and the production terms in the *k*-ε turbulence model are largely responsible for the differences between the wave-induced longshore current predicted by the 2DH and 3D model. As these are physical processes, it was concluded that computations with the 3D model are more accurate for the wave-driven longshore currents in the surf zone. The effect of the wave angle and the cross-shore location on the difference between 2DH and 3D model computations is discussed further in Treffers (in preparation).

As a consequence, a calibrated 2DH model cannot be transferred into a 3D model without re-calibration of the hydrodynamics. The same applies when changing the number of vertical layers. The latter is not very practical, and this can possibly be circumvented by computing the bed shear stress on the basis of a velocity at a particular elevation above the bed, independent of the layer distribution, e.g. at the (computed) edge of the wave boundary layer.

Figure 4.9 proves the necessity to re-calibrate the 3D model. This has been done by increasing the Chézy roughness coefficient (decreasing the roughness) such that the agreement between the measured and computed longshore current velocities is closest. This results in C = 75 $m^{0.5}/s$, which corresponds in case of a logarithmic current profile to roughness heights of k_s = 2.0*10^{-4} m, 1.0*10^{-4} m and 0.5*10^{-4} m for water depths of 8 m, 4 m and 2 m, respectively. This corresponds to very smooth seabeds. Considering the typical bed grain size (2.0*10^{-4} m) and the bed was locally covered with small-scale bedforms inducing form roughness, this low roughness appears to be physically unrealistic. However, this low roughness is necessary to get a reasonable agreement with the measured longshore current data, compensating for model limitations.

Figure 4.10 shows a comparison between measured and computed longshore current velocities with the 3D model with a roughness coefficient of 75 $m^{0.5}/s$. The left panel shows the computed velocities at the measurement elevation, the right panel the depth-averaged velocities. This figure indirectly shows that the difference between the depth-averaged and the velocity and the measurement elevations is small, as was expected (see Section 2.2). Compared to the 2DH model (see Figure 3.2), agreement between computations and measurements is worse. This is surprising; one would expect the opposite since the 3D model contains more physics (e.g. undertow, vertical viscosity profile). The comparison is probably also not unbiased, since the 2DH model has been calibrated more thoroughly than the 3D model. Therefore, it is recommended to carry out a thorough model validation based on velocity profile data. The data used in Reniers et al. (2004) could be used for this purpose.

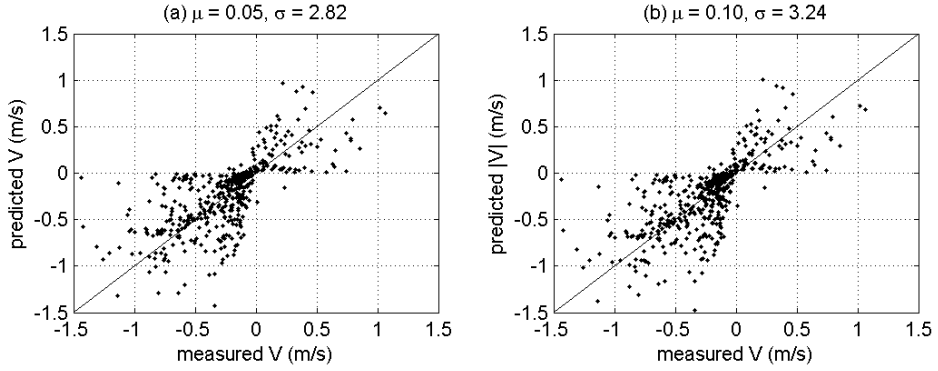

Figure 4.10 Comparison between measured and computed (3D model) longshore current velocities. Panel (a) shows the computed velocities at the measurement elevation, panel (b) the depth-averaged computed velocities.

Figure 4.11 shows that the 3D model predicts the location of the longshore current maxima too far onshore, even more than the 2DH model does (Figure 3.15). The magnitude of the longshore current maxima is, however, better predicted by the 3D than by the 2DH model.

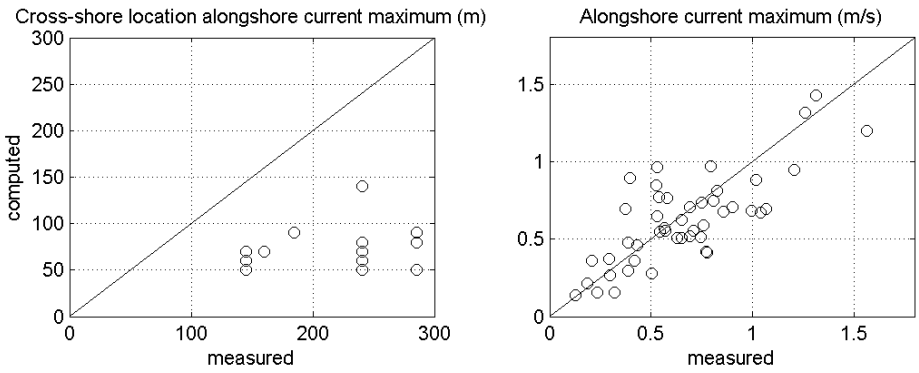

Figure 4.11 Comparison between measured and computed (3D model) cross-shore location and magnitude of the longshore current maximum.

Chapter 5 Conclusions and recommendations

5.1 Conclusions

We have compared 2DH and 3D Delft3D computations with measured wave and current data in the nearshore zone for 46 SandyDuck97 cases. Furthermore, we have tested the sensitivity of the 2DH model predictions to the Chézy roughness coefficient *C*, the background horizontal viscosity $v_{h,back}$, including breaker delay and the breaking wave dissipation coefficient α in the roller model. Finally, we have tested the effect of the turbulence model and the number of vertical computational layers on the longshore currents predicted by the 3D model. From this we conclude the following.

1 The Chézy roughness coefficient and the background horizontal viscosity hardly affect the Delft3D wave height predictions, but do have a strong effect on the current predictions. Breaker delay and the wave dissipation coefficient have a larger impact on the wave height predictions in the surf zone where wave breaking is dominant, and therefore also indirectly on the current predictions. Best agreement between measured and predicted (2DH model) wave heights and longshore currents is obtained with C = 60 $m^{0.5}/s$, $v_{h,back}$ = 0.0 m^2/s, no breaker delay and α = 1.0.

2 With these model settings, the 2DH model is able to predict the wave heights reasonably well (mean relative error 0.08, standard deviation relative error 0.11). However, wave heights are systematically overpredicted, which could be related to the absence of wave dissipation due to bottom friction in the roller model.

3 The mean relative error of the longshore current predictions by the 2DH model is close to zero; partly because the model was calibrated on these measured data. The standard deviation is rather large (2.3); currents are generally overpredicted at deep water and underpredicted at shallow water. The 2DH model overpredicts the longshore current maxima and underpredicts the distance of these maxima to the shore.

4 The longshore current predictions with the 3D model proved to be very sensitive to the adopted turbulence model and the number of vertical computational layers, or more specific the thickness of the lowest computational layer. For wave-driven currents, the *k*-ε model is expected to give better predictions of the current profile, as it contains more physics. The thinner the lowest computational layer, the lower the longshore currents. This is related to the way the bed shear stress is calculated and/or inconsistencies between bottom boundary conditions of the turbulence model and the bed shear stress.

5 The depth-averaged currents computed by the 3D model are systematically lower than those computed by the 2DH model. Therefore, a 3D model based on an 2DH model needs to be re-calibrated hydrodynamically. This was done by increasing the Chézy roughness coefficient from 60 $m^{0.5}/s$ to 75 $m^{0.5}/s$, which corresponds to a physically unrealistic smooth bed. The calibrated 3D model performs worse than the 2DH model in predicting the longshore currents and the location of the longshore current maxima, but does better in predicting the magnitude of the longshore current maxima.

5.2 Recommendations

Based on this study we recommend the following.

1 Add wave dissipation due to bottom friction as a sink term to the expression for the short wave energy in the roller model. This could improve wave height predictions at deeper water.

2 Compute the bed shear stress using the velocity at the edge of the wave boundary layer instead of the velocity in the lowest computation layer to circumvent the dependency of computed longshore currents on the thickness of the lowest computational layer.

3 Investigate how well Delft3D is able to compute the vertical flow structure of wave-driven currents using the field data of Reniers et al. (2004).

4 Study the capability of Delft3D to compute wave-driven longshore currents in isolation of other forcings (wind, tide). For this purpose, the laboratory data of Visser (1984) and Reniers (1997) could be used.

5 Study how well Delft3D can simultaneously predict longshore and cross-shore wave-induced currents by calibration against above-mentioned data sets.

6 Use the same data to investigate (i) whether a 3D Delft3D model better predicts the depth-averaged wave-induced longshore currents than a 2DH model and (ii) at which conditions a 2DH model is sufficient.

7 Critically review how wave-induced turbulence is modelled in Delft3D.

8 Investigate the contribution of the roller dissipation to the horizontal eddy viscosity. This may play an important role in the horizontal (cross-shore) distribution of the wave-driven current.

9 Investigate the effect of the β_{roller} parameter.

Chapter 6 Acknowledgements

The author wishes to thank Drs. Birkemeier, Long, Hathaway, Elgar, Guza and Herbers for providing the SandyDuck97 datasets. Larry Hsu is very much acknowledged for providing his report and sharing his Delft3D model of the SandyDuck cases.

Chapter 7 References

Birkemeier, W.A., Thornton, E.B., 1994. The DUCK94 nearshore field experiment. Proceedings Coastal Dynamics Conference, Barcelona, Spain, pp. 815-821.

Hsu, Y., J.D. Dykes, R.A. Allard and J.M. Kaihatu 2006. Evaluation of Delft3D Performance in Nearshore Flows. NRL memorandum report, NRL/MR/7320-06-8984, Naval Research Laboratory, USA.

Hsu, Y., J.D. Dykes, R.A. Allard and D.W. Wang, 2006. Validation Test Report for Delft3D. NRL memorandum report, NRL/MR/7320-08-9079, Naval Research Laboratory, USA.

Luijendijk, A. 2007. Wave-driven longshore current 2DH vs. 3D. Memo, WL|Delft Hydraulics, The Netherlands.

Reniers, A.J.H.M., Battjes, J.A., 1997. A laboratory study of longshore currents over barred and non-barred beach. Coastal Engineering, 30: 1-22.

Reniers, A.J.H.M., J.A. Roelvink and E.B. Thornton, 2004. Morphodynamic modelling of an embayed beach under wave group forcing. Journal of Geophysical Research, 109, C01030.

Reniers, A.J.H.M., Thornton, E.B., Stanton, T.P., Roelvink, J.S., 2004. Vertical flow structure during Sandy Duck: observations and modelling. Coastal Engineering, 51: 232-260.

Roelvink, J.A., Th.J.G.P. Meijer, K. Houwman, R. Bakker, R. Spanhoff, 1995. Field validation and application of a coastal profile model. Proceedings Coastal Dynamics Conference, Gdansk, Poland, pp. 818-828.

Ruesink, B.G., D.J.R. Walstra and H.N. Southgate, 2003. Calibration and verification of a parametric wave model on barred beaches. Coastal Engineering, 48: 139-149.

Savioli, J.C., 2000. Turbulence and sediment transport. A numerical investigation. Ph.D. thesis, University of Twente, The Netherlands.

Treffers, R., in preparation. Validation hydrodynamics Delft3D. Comparison of 2D and 3D models. M.Sc. thesis, Technical University of Delft, The Netherlands.

Van Rijn, L.C., 2007a. Unified view of sediment transport by currents and waves. I: Initiation of motion, bed roughness, and bed-load transport. Journal of Hydraulic Engineering, 133: 649-667.

Van Rijn, L.C., 2007b. Unified view of sediment transport by currents and waves. II: Suspended transport. Journal of Hydraulic Engineering, 133: 668-689.

Van Rijn, L.C., 2007c. Unified view of sediment transport by currents and waves. III: Graded beds. Journal of Hydraulic Engineering, 133: 761-775.

Visser, P.J., 1984. Uniform longshore current measurements and calculations. Proceedings 19th International Conference on Coastal Engineering, New York, USA, pp. 11,845-11,856.

Walstra, D.J.R., 2000. Unibest-TC Userguide. Research Report Z2897, WL|Delft Hydraulics, The Netherlands.

Walstra, D.J.R., C. Brière, A.B. Cohen, A.R. van Dongeren, I.J.P. Elshoff, C. Hoyng, M. van Ormondt, S. Quartel, B. de Sonneville, P.K. Tonnon, L. Uunk, 2008. Monitoring and Modelling of a surface nourishment. VOP Short Term Morphology. Research Report Z4479, WL|Delft Hydraulics, The Netherlands.

Appendix A MDF-file Delft3D model SandyDuck97 cases

```
Ident = #Delft3D-FLOW  .03.02 3.39.28#
Commnt=
Runtxt= #SandyDuck Regular rectangular #
      #grid                    #
Filcco= #flow2.grd#
Fmtcco= #FR#
Anglat=  3.6000000e+001
Grdang=  0.0000000e+000
Filgrd= #flow2.enc#
Fmtgrd= #FR#
MNKmax= 87 118 10
Thick =  0.4600000e+001
       0.6400000e+001
       0.9000000e+001
       1.2500000e+001
       1.7500000e+001
       1.7500000e+001
       1.2500000e+001
       0.9000000e+001
       0.6400000e+001
       0.4600000e+001
Commnt=
Fildep= #flow2.dep#
Fmtdep= #FR#
Commnt=
Commnt=                        no. dry points: 0
Commnt=                        no. thin dams: 0
Commnt=
Itdate= #1997-10-18#
Tunit = #M#
Tstart=  7.8000000e+002
Tstop =  8.4000000e+002
Dt    = 0.100000001
Tzone = 0
Commnt=
Sub1  = #  W #
Sub2  = #  W#
Commnt=
Wnsvwp= #N#
Filwnd= #du8.wnd#
Fmtwnd= #FR#
Wndint= #Y#
Commnt=
Zeta0 =  0.0000000e+000
U0    = [.]
V0    = [.]
S0    = [.]
Commnt=
Commnt=                        no. open boundaries: 3
```

```
Filbnd= #du8.bnd#
Fmtbnd= #FR#
FilbcT= #du8.bct#
FmtbcT= #FR#
Commnt=
Ag    =  9.8100004e+000
Rhow  =  1.0250000e+003
Alph0 = [.]
Tempw =  1.5000000e+001
Salw  =  3.1000000e+001
Rouwav= #FR84#
Wstres=  6.3000002e-004  0.0000000e+000  7.2300001e-003  1.0000000e+002
Rhoa  =  1.0250000e+000
Betac =  5.0000000e-001
Equili= #N#
Tkemod= #TkeModKey   #
Ktemp = 0
Fclou =  0.0000000e+000
Sarea =  0.0000000e+000
Temint= #Y#
Commnt=
Roumet= #C#
Ccofu =  Ckey
Ccofv =  Ckey
Xlo   =  0.0000000e+000
Vicouv=  VicouvKEY
Dicouv=  1.0000000e+001
Htur2d= #N#
Irov  = 0
Commnt=
Iter  =      2
Dryflp= #YES#
Dpsopt= #MEAN#
Dpuopt= #MEAN#
Dryflc=  2.0000000e-001
Dco   = -9.9900000e+002
Tlfsmo=  1.5000000e+001
ThetQH=  0.0000000e+000
Forfuv= #Y#
Forfww= #N#
Sigcor= #N#
Trasol= #Cyclic-method#
Momsol= #Cyclic#
Commnt=
Commnt=                 no. discharges: 0
Commnt=                 no. observation points: 11
Filsta= #du8.obs#
Fmtsta= #FR#
Commnt=                 no. drogues: 0
Commnt=
Commnt=
Commnt=                 no. cross sections: 0
Commnt=
```

SMhydr= #YYYYY#
SMderv= #YYYYYY#
SMproc= #YYYYYYYYYY#
PMhydr= #YYYYYY#
PMderv= #YYY#
PMproc= #YYYYYYYYYY#
SHhydr= #YYYY#
SHderv= #YYYYY#
SHproc= #YYYYYYYYYY#
SHflux= #YYYY#
PHhydr= #YYYYYY#
PHderv= #YYY#
PHproc= #YYYYYYYYYY#
PHflux= #YYYY#
Online= #N#
Waqmod= #N#
WaveOL= #Y#
Prhis = 0.0000000e+000 0 1.2000000e+002
Flmap = 7.8000000e+002 60 8.4000000e+002
Flhis = 7.8000000e+002 3 8.4000000e+002
Flpp = 7.8000000e+002 30 8.4000000e+002
Flrst = 0
Commnt=
Cstbnd= #yes#
Roller= #yes#
Gamdis= -1.
F_lam = FlamKEY
Alfaro= AlfaroKey
Commnt=

Appendix B MDW-file Delft3D model SandyDuck97 cases

```
Delft3D WAVE GUI version 4.92.00
*
********** Datagroup Description ***************************************
*
* Project name
'SandyDuck'
* Project number
''
* Description
'Regular Rec. grids -3.25.04'
''
''
*
********** Datagroup Hydrodynamics *************************************
*
* Y/N Use bathmetry, use waterlevel, use current, use wind
0 1 1 1
*
********** Datagroup Grids *********************************************
*
* Number of computational grids
1
* Filename computational grid
'swan2.grd'
* Y/N bathymetry is based on computational grid, filename bathymetry grid
1 ''
* Filename bathymetry data
'swan2.dep'
* Directional space: type, number of directions,
*                    start-direction, end-direction
*   - type: 1 = circle, 2 = sector
1 36  0.0000000e+000  0.0000000e+000
* Frequency space: lowest frequency, highest frequency, number of frequency bins,
*                  grid to nest in, Y/N write output for this grid
 5.0000001e-002  3.4999999e-001 25 0 1
*
********** Datagroup Time frame ****************************************
*
* Number of tidal time points, Reference date
1 1997-10-18
* Time, h, u, v
 7.8000000e+002  0.0000000e+000  0.0000000e+000  0.0000000e+000
* Water level correction, extend flow data on the last # grid(s),
* extend bathymetry, water level, current, wind
 0.0000000e+000 1 0 1 1 1
*
********** Datagroup Boundaries ****************************************
*
* Number of boundaries
```

```
3
* Boundary name, specifications, defined-by, conditions-along-boundary
*   - specifications: 1 = from-file, 2 = parametric
*   - defined-by: 1 = orientation,
*                 2 = grid-coordinates,
*                 3 = xy-coordinates
*   - conditions-along-boundary: 1 = uniform, 2 = space-varying
'Boundary 1' 1 1 1
* Orientation
*   1 = N, 2 = NW, 3 = W, 4 = SW, 5 = S, 6 = SE, 7 = E, 8 = NE
1
* Filename for boundary conditions
'spcnorth.bnd'
* Boundary name, specifications, defined-by, conditions-along-boundary
*   - specifications: 1 = from-file, 2 = parametric
*   - defined-by: 1 = orientation,
*                 2 = grid-coordinates,
*                 3 = xy-coordinates
*   - conditions-along-boundary: 1 = uniform, 2 = space-varying
'Boundary 2' 1 1 1
* Orientation
*   1 = N, 2 = NW, 3 = W, 4 = SW, 5 = S, 6 = SE, 7 = E, 8 = NE
7
* Filename for boundary conditions
'spceast.bnd'
* Boundary name, specifications, defined-by, conditions-along-boundary
*   - specifications: 1 = from-file, 2 = parametric
*   - defined-by: 1 = orientation,
*                 2 = grid-coordinates,
*                 3 = xy-coordinates
*   - conditions-along-boundary: 1 = uniform, 2 = space-varying
'Boundary 3' 1 1 1
* Orientation
*   1 = N, 2 = NW, 3 = W, 4 = SW, 5 = S, 6 = SE, 7 = E, 8 = NE
5
* Filename for boundary conditions
'spcsouth.bnd'
*
********** Datagroup Obstacles ****************************************
*
* Number of obstacles
0
*
********** Datagroup Physical parameters ******************************
*
* Gravity, water density, north, minimum depth
 9.8100004e+000  1.0250000e+003  9.0000000e+001  5.0000001e-002
* Convention, set-up, forces
*   - convention: 1 = nautical, 2 = cartesian
*   - set-up: 0 = no set-up, 1 = activated
*   - forces: 1 = radiation stress, 2 = wave energy dissipation rate
1 0 2
* Type of formulations
```

```
*   0 = none, 1 = 1st, 2 = 2nd, 3 = 3rd generation
3
* Depth induced breaking, alpha, gamma
*   - breaking: 0 = de-activated, 1 = B&J model
1  1.0000000e+000  7.3000002e-001
* Bottom friction, friction coefficient
*   - friction: 0 = de-activated, 1 = Jonswap,
*               2 = Collins, 3 = Madsen et al.
1  6.7000002e-002
* Non-linear triad interactions, alpha, beta
*   - interactions: 0 = de-activated, 1 = LTA
0  1.0000000e-001  2.2000000e+000
* Diffraction, smoothing coefficient, smoothing steps, adaptation of propagation
*   - interactions: 0 = de-activated, 1 = activated
0  2.0000000e-001 5 1
* Y/N windgrowth, white-capping, quadruplets, refraction, frequency shift
1 1 1 1 1
*
********** Datagroup Numerical parameters ******************************
*
* Directional space, frequency space
 5.0000000e-001  5.0000000e-001
* Hs-Tm01, Hs, Tm01, percentage of wet grid points, maximum number of iterations
 2.0000000e-002  2.0000000e-002  2.0000000e-002  9.8000000e+001 15
*
********** Datagroup Output curves *************************************
*
* Number of output curves
0
*
********** Datagroup Output parameters *********************************
*
* Level of test output, debug level, Y/N compute waves, Y/N activate hotstart file
* Output time interval, Computational mode: 0 = stationary, 1 = non-stationary
0 0 1 0  3.0000000e+001 0
* Y/N output to Flow grid; filename of Flow grid
1 'flow2.grd'
* Y/N output to locations
1
* Output locations: 1 = from file, 2 = parametric
2
* Number of locations
1
* X-Y location co-ordinates
 8.8000000e+002  9.2200000e+002
* Y/N table, 1D-spectra, 2D-spectra
1 0 1
```